DEVELOPMENT AND PROCESS EVALUATION OF IMPROVED FISCHER-TROPSCH SLURRY CATALYSTS

QUARTERLY TECHNICAL PROGRESS REPORT

FOR THE PERIOD 1 APRIL TO 30 JUNE 1987

August 25, 1987

by

Howard P. Withers

Air Products and Chemicals, Inc.

Allentown, PA 18105

and

Dragomir B. Bukur and Michael P. Rosynek

Departments of Chemical Engineering and Chemistry

Texas A&M University

College Station, TX 77843

WORK PERFORMED UNDER DOE CONTRACT NO. DE-AC22-85PC80011

FOR THE UNITED STATES DEPARTMENT OF ENERGY

THE PITTSBURGH ENERGY TECHNOLOGY CENTER

PITTSBURGH, PENNSYLVANIA

DEVELOPMENT AND PROCESS EVALUATION OF IMPROVED FISCHER-TROPSCH SLURRY CATALYSTS

QUARTERLY TECHNICAL PROGRESS REPORT

FOR THE PERIOD 1 APRIL TO 30 JUNE 1987

August 25, 1987

by

Howard P. Withers

Air Products and Chemicals, Inc.

Allentown, PA 18105

and

Dragomir B. Bukur and Michael P. Rosynek

Departments of Chemical Engineering and Chemistry

Texas A&M University

College Station, TX 77843

WORK PERFORMED UNDER DOE CONTRACT NO. DE-AC22-85PC80011-3

FOR THE UNITED STATES DEPARTMENT OF ENERGY

THE PITTSBURGH ENERGY TECHNOLOGY CENTER

PITTSBURGH, PENNSYLVANIA

DISCLAIMER

Project Manager - Sweenam R. Lee
Liquid Fuels Division
Pittsburgh Energy Technology Center
Pittsburgh, Pennsylvania

Program Manager - John Shen
Office of Coal Preparation & Liquefaction
Department of Energy
Washington, DC

TABLE OF CONTENTS

I. ABSTRACT

During this reporting period three runs were made with a commercial fused iron catalyst (from United Catalysts, Inc., C73-1) with objectives to study the effects of catalyst reduction procedure, particle size and process conditions on fixed bed reactor performance (activity and product selectivity). It was found that the catalyst activity increases as the space velocity of H_2 during the reduction increases or as the catalyst particle size decreases. Also, these parameters have some effect on the product selectivity.

An uncalcined precipitated iron catalyst (100 Fe/1 Cu/0.2 K on weight basis) synthesized in our laboratory was evaluated in a fixed bed reactor. Initially, it showed an activity more than twice of the fused iron catalyst, but it deactivated after about 30 hours on stream. The deactivation can be attributed to the presence of a "hot spot" in the bed during this initial period.

The work on catalyst synthesis and characterization of the precipitated iron catalysts has continued. A total of 25 precipitated iron catalysts (Fe/Cu, Fe/K and Fe/Cu/K) have been prepared in batches of approximately 100 g each. Temperature programmed reduction has revealed that the iron reduction is facilitated in the presence of copper. Also, two catalysts, unpromoted iron and potassium promoted iron (containing 1 part K per 100 parts Fe) were examined using Fourier Transform Infrared Spectroscopy.

II. OBJECTIVE AND SCOPE OF WORK

The objective of this contract is to develop a consistent technical data base on the use of iron-based catalysts in Fischer-Tropsch synthesis reactions. This data base will be developed to allow the unambiguous comparison of the performance of these catalysts with each other and with state-of-the-art iron catalyst compositions. Particular attention will be devoted to generating reproducible kinetic and selectivity data and to developing reproducible improved catalyst compositions. To accomplish these objectives, the following specific tasks will be undertaken.

TASK 1 - Project Work Plan

The objective of this task is to establish a detailed project work plan covering the entire period of performance of the contract. This includes estimated costs and manhours expended by month for each task.

TASK 2 - Slurry Catalyst Improvement

The primary purpose of this task is to develop improved iron-based catalysts, both precipitated and supported, that show enhanced activity and selectivity in slurry phase testing. This will be accomplished by gaining systematic understanding of the role of promoters, binders, supports and activation procedures in determining the activity and selectivity of iron-based catalysts. The catalyst development program will incorporate extensive physical and chemical characterization of these materials with the objective to establish correlations between the physical/chemical properties of these catalysts and the corresponding catalytic behavior for synthesis gas conversion.

TASK 3 - Process Evaluation Research

The purpose of this task is to subject the most improved catalysts (based on activity and selectivity) to a thorough process evaluation. This involves long term stability studies, investigation of a wide range of process variables, and determination of kinetic parameters. These kinetic parameters will be utilized to simulate catalyst performance under actual bubble column conditions.

TASK 4 - Economic Evaluation

The aim of this task is to develop the relative economic impact for each improved catalyst composition and compare these economics with the economics of using the base case catalyst. Data obtained from Tasks 2 and 3 will be used to generate a product yield structure, Fischer-Tropsch reactor residence time, and key process flow rates. These economic studies will include relative capital costs, operating costs, and required revenues for each catalyst, as well as a sensitivity study of the assigned relative values of the principal products (i.e. diesel and gasoline).

III. SUMMARY OF PROGRESS

During the third quarter of this contract three runs with a commerical fused iron ammonia synthesis catalyst (C73-1 from United Catalysts, Inc.) were made in a fixed bed reactor to investigate effects of H_2 space velocity during the reduction, catalyst particle size and process conditions on the catalyst activity and product selectivity.

It was found that the catalyst reduced at higher H_2 space velocity (20,000 h^{-1} based on the catalyst volume; Run FA-01-1537 with 30/60 mesh particles) is more active (25-43% higher space-time-yield) than the catalyst reduced at a lower space velocity (10,000 h^{-1}, Run FA-01-1147 with 30/60 mesh particles). Test conditions were 1.6 MPa (215 psig), H_2/CO feed ratio of 1:1, 0.75 Nℓ/g·cat/h and temperatures of 235, 250 and 265°C. The use of higher H_2 space velocity during the reduction results in somewhat higher yields of lighter hydrocarbons and oxygenates whereas there are no changes in the methane selectivity and olefin content of the products.

The effect of particle size was studied in runs FA-01-1537 (30/60 mesh particles) and FA-01-1417 (60/100 mesh particles) under the same process conditions as given above. Higher activities (up to 29% in terms of the space-time-yield) were obtained with smaller particles, which indicates that intraparticle diffusional limitations are significant. Product selectivities were similar, except that olefin to paraffin ratios and the yield of oxygenates were slightly higher in runs with the smaller catalyst particles.

In run FB-01-1547 with 170/230 mesh particles two mass balances were made under the process conditions used by workers at Exxon (Satterfield *et al.*, 1985), 0.79 MPa (100 psig), H_2/CO feed ratio of 1:1, 1.5 Nℓ/g·cat/h

and temperatures of 234 and 245°C. The catalyst activity was about 10% lower than that reported by Exxon workers, but C_2-C_4 olefin to paraffin ratios obtained in our study were much higher than those obtained at Exxon (C_2 : 4.2 vs. 0.15; C_3: 5.8 vs. 0.8; C_4: 4.4 vs. 0.9). However, our values are very similar to values obtained at MIT in a slurry reactor (Satterfield *et al.*, 1985) under the same process conditions, but with H_2/CO feed ratio of 0.9.

One run was made with an uncalcined sample of a precipitated iron catalyst (100Fe/1 Cu/0.2 K on weight basis) which was synthesized in our laboratory. The catalyst (gas hourly space velocity of 3,200h^{-1} based on volume of the catalyst) was reduced using synthesis gas with H_2/CO = 0.7 at 280°C, atmospheric pressure, space velocity of 4Nℓ/g·Fe/h for 8 hours. After 27 hours on stream at 1.6 MPa, 2.5 Nℓ/g·cat/h, 235°C and H_2/CO = 1.0 the catalyst exhibited high activity: CO conversion of 48% and the space-time-yield of 54 mols syngas converted per kilogram of catalyst per hour. A "hot spot" with ~20°C higher temperature than the rest of the bed developed during the first balance, and in the next three balances at lower space velocities or at higher temperature (250°C) much lower activity was obtained due to catalyst deactivation. During the first balance the hydrocarbon selectivities were C_1: 3.3%; C_2-C_4: 14.2%; C_5-C_{11}: 18.7% and C_{12}^+: 63.8% on weight basis.

Construction of a new fixed bed reactor apparatus has been completed, and the unit has been successfully tested (Run FB-01-1547). A detailed design of the data acquisition/computer control system for a new slurry reactor system has been completed.

A total of 25 different unsupported iron precipitated catalysts have been synthesized (~100g of each). Temperature programmed reduction studies for Fe/Cu catalysts have revealed that the presence of copper facilitates reduction of iron. Also, the presence of even small amounts of potassium (0.05%) in copper free catalysts significantly increases the extent of reduction of Fe_3O_4 to metalic iron.

Physical adsorption measurements performed thus far, using N_2 at -196°C, indicated that the surface areas of the "as prepared" (i.e. un-calcined, unreduced) catalysts tend to increase with increasing copper content (180 m^2/g for iron without any copper, 370 m^2/g for catalyst with 20 grams of Cu per 100 g of Fe). However, all of the catalysts, regardless of Cu level, exhibit marked decrease in surface area after calcination in air at 300°C or after H_2 treatment for 4 hours at 300°C and gas hourly space velocity of 3500 h^{-1}. After these treatments the surface areas are between 7 and 10m^2/g.

Fourier Transform Infrared Spectroscopy has been used to obtain information about the surface properties of the precipitated iron catalysts, using nitric oxide as a probe molecule. An unpromoted iron catalyst, and a potassium promoted iron catalyst (containing 1 part K per 100 parts Fe) were examined with this technique. Both materials were found to yield similar results.

IV. DETAILED DESCRIPTION OF TECHNICAL PROGRESS

TASK 1 - Project Work Plan

The project work plan was completed during the first quarter of this project and the detailed work plan was submitted to APCI.

TASK 2 - Slurry Catalyst Improvement

2.1 Design and Construction of Reactor Systems

2.1.1 Fixed Bed Reactor Apparatus

The existing fixed bed reactor apparatus (Unit A) was modified by addition of a preheater upstream of the reactor and a high temperature/high pressure collection trap downstream of the reactor. The preheater is a cylindrical vessel filled with alumina particles wrapped with a heating tape around its circumference. The outlet temperature is monitored with a thermocouple, and power is supplied via a variable voltage transformer. The addition of the preheater facilitates temperature control of the reactor and the addition of the hot collection trap (maintained at 180-210°C) helps prevent condensation of heavy molecular weight products in lines and the back pressure regulator.

Construction of the new fixed bed reactor apparatus (Unit B) has been completed. This unit is similar to the existing fixed bed reactor unit, and its flow diagram and description were given in the Technical Progress Report for the period October 17, 1986-January 31, 1987. Following construction, a blank run was performed to determine whether the reactor walls have appreciable F-T activity. The reactor was filled with 60/100 mesh glass beads and exposed to flowing hydrogen at atmospheric pressure and 400°C for 24 hours ("activation" period). After that a synthesis gas feed (H_2/CO = 1:1) was introduced at a flow rate of 60 ml/min (STP), and the

reactor temperature and pressure were 300°C and 400 psig, respectively. The system was held at these conditions for 24 hours, and the (H_2 + CO) conversion was approximately 1.5%. This level of activity is quite small and will have negligible effect on results during catalyst evaluations.

2.1.2 Slurry Bed Reactor Apparatus

A detailed design of the data acquisition/computer control system for a new slurry reactor apparatus (slurry reactor B) has been completed. Construction is scheduled to be completed during the next quarter.

2.2 Product Analysis System

Some preliminary work on wax analysis has been initiated using a 10 m x 0.53 mm ID wide bore capillary column coated with polydimethyl silicone (RSL-150 from Alltech Associates) and an on-column injector. Samples of a hard paraffin wax (designated FT-300, from Durachem Commodities, New York) were dissolved in toluene, and good separation up to about carbon number 50 was obtained. Additional studies aimed at optimizing this procedure will be undertaken during the next quarter and a detailed description of the method will be presented.

2.3 Catalyst Testing in Fixed Bed Reactors

During the previous quarter a fused iron catalyst used for ammonia synthesis (United Catalysts, Inc., C73-1) was evaluated in both the slurry and the fixed bed reactor under the same process conditions. In these tests it was found that the space-time-yield (expressed as moles syngas converted per gram of catalyst per hour) is higher in the slurry reactor than in the fixed bed reactor. This is not in agreement with results reported by Satterfield et al. (1985), who used the same catalyst but much smaller catalyst particles in their fixed bed reactor experiments (170/230

mesh vs. 30/60 mesh employed in our run FA-01-1147). In order to determine the effects of particle size and activation procedure on the performance of this catalyst, and to gain additional experience with operation of a fixed bed reactor, three runs with the fused iron catalyst (C73-1) were made. In all cases the same in-situ reduction procedure was employed (see Appendix I for details). This procedure differs from the one described in the previous quarterly report in that a higher H_2 gas hourly space velocity was employed (20,000 vs. 10,000 h^{-1}). This space velocity was chosen to be the same as that used by workers at Exxon as reported by Satterfield et al. (1985). The bed was diluted with glass beads of the same particle size as the catalyst in the ratio 4:1 (inert:catalyst on a volume basis) in an attempt to prevent development of hot spots during the reactor operation.

Also, one run was made with a precipitated iron catalyst prepared in our laboratory according to the procedure described in the Quarterly Report, January - March, 1987. An uncalcined sample of this catalyst having composition 100Fe/1 Cu/0.2K, on a weight basis, was reduced at atmospheric pressure with the syngas mixture ($H_2/CO = 0.7$) for 8 hours. (Details of the reduction procedure are given in Appendix I)

A detailed discussion of results obtained with the fused and the precipitated iron catalyst is given below.

2.3.1 Run FA-01-1537 (30/60 mesh fused iron catalyst)

The purpose of this run was to determine the effect of H_2 space velocity (20,000 h^{-1} vs. 10,000 h^{-1}) during reduction on catalyst performance. Three mass balances were performed using the same process conditions as in the previous run with this catalyst (FA-01-1147), i.e. P = 1.59 MPa (215 psig), SV = 0.75 Nℓ/g-cat/h (2,000 h^{-1} based on the volume of

catalyst only), H_2/CO feed ratio of 1:1 and temperatures of 235, 250 and 265°C. Selected results are summarized in Table 1.

The catalyst activity, expressed in terms of the syngas and CO conversions or the space-time-yield, increases with temperature as well as the yield of light products, both of which is as expected. At 265°C, carbon monoxide is almost completely consumed (98% conversion) and the syngas conversion is about 86%. The yield of wax (which is defined as the product collected in the high temperature trap) during the first mass balance period at 235°C was unexpectedly low, which was probably caused by the fact that the system had not yet reached steady-state. Products that were collected in the cold trap follow the Anderson-Schulz-Flory (ASF) distribution up to about C_{13}, with subsequent tailing of the products as shown in Figure 1 (mass balance period 3). The reason for this tailing is that products collected in a high temperature (180-220°C)/high pressure trap, which are mostly high molecular weight hydrocarbons, were not analyzed. Similar results were obtained in the other two mass balances and a value of the chain growth probability factor of the ASF distribution was nearly the same for all three balances (α = 0.68-0.70). The system operation during this run was very stable and nearly isothermal conditions were achieved at all operating temperatures. No signs of catalyst deactivation were observed and the run was arbitrarily terminated after 72 hours of operation.

Results from this run and run FA-01-1147 (Quarterly Report, February-April, 1987) which illustrate the effect of H_2 space velocity during the reduction on the catalyst activity and selectivity are given in Table 2. Some general observations that are valid for all three temperatures are as

follows. The catalyst reduced at higher space velocity (FA-01-1537) has significantly higher activity (25-43% higher space-time-yield) and gives higher yields of light hydrocarbons and oxygenates. Methane yields and olefin to paraffin ratios of low molecular weight hydrocarbons are not strongly affected by H_2 space velocity during the reduction.

2.3.2 Run FA-01-1417 (60/100 mesh fused iron catalyst)

The catalyst used in this run was reduced at a high space velocity (20,000 h^{-1} based on volume of the catalyst) and the main purpose of the run was to determine the effect of particle size (60/100 mesh vs. 30/60 mesh) on catalyst activity and product selectivity. Six mass balances were performed during this run, five of which were at the same conditions used in the previous runs with the same catalyst, i.e. P = 1.6 MPa, 0.75 Nℓ/g-cat/h, H_2/CO = 1.0 and temperatures of 235, 250 and 265°C, whereas one balance was made at 0.79 MPa, 233°C, 1.5 Nℓ/g-cat/h with the synthesis gas feed with H_2 to CO molar ratio of 1:1. Selected results are given in Table 3.

The first mass balance was made after about 40 hours on stream at 1.6 MPa, 235°C and 0.75 Nℓ/g-cat/h and the observed H_2 + CO and CO conversions, 73.1% and 83.9%, were much higher than in the run FA-01-1537 (balance 1), which under the same conditions were 52.2% and 60.4%, respectively. This shows that intraparticle diffusional limitations were present in the run with 30/60 mesh particles. The second balance was made at lower pressure, 0.79 MPa, and these results will be discussed together with those obtained with 170/230 mesh particles later in the report (Table 5). In the next two balances the temperature was increased to 250°C and 265°C respectively, which was accompanied with increase in catalyst activity and light hydro-

carbon yields and selectivity, whereas the wax yield and selectivity decreased with the increase in temperature. (H_2 + CO) and CO conversions changed only slightly when the temperature was raised from 250 to 265°C, because CO was almost completely consumed at 250°C. After the mass balance at 265°C the temperature was reduced to 250°C (period 5) and some catalyst deactivation was observed. CO conversion during this balance was 81%, which is significantly lower than that obtained during the third mass balance period (97%). Catalyst deactivation was also observed upon returning to initial conditions at the end of the run (balance 6). In this case CO conversion was only 47% compared to 84% obtained during the first mass balance. As a result of deactivation, hydrocarbon selectivity shifts towards lighter hydrocarbons, e.g. at 235°C, C_2-C_4 and C_5-C_{11} selectivities were 35.3 and 41.6% (balance 6), whereas during the balance 1 they were 26.6 and 31.1%, respectively.

ASF plots for the mass balance periods 1, 3 and 4 are shown in Figures 2-4. Products collected in the high temperature/high pressure trap were combined with the organic phase products collected in a cold trap (0°C and atmospheric pressure) during the first mass balance period, but not during others. The product distribution for the first balance can be described reasonably well by two straight lines on the ASF plot: one for products in C_1-C_{10} range with a corresponding value for α of 0.74, and one for products in the range C_{11} - C_{25} with α = 0.87. This type of behavior has been found in several previous studies with this catalyst, as well as with precipitated iron catalysts (Bauer *et al.*, 1983, Huff and Satterfield, 1984; Egiebor and Cooper, 1985). For the other two balances (3 and 4) the products collected in the cold trap follow the ASF distribution up to C_{11}

(period 4) or C_{13} (period 3). After these negative deviations from the ASF occur. Again, these negative deviations from the ASF distribution are due to the fact that the entire product spectrum was not analyzed.

Results from runs FA-01-1417 (60/100 mesh) and FA-01-1537 (30/60 mesh) which illustrate the effect of particle size on catalyst activity and selectivity are shown in Table 4. Results from the slurry reactor run SA-01-0817 (Quarterly Report January - March 1987) are also included for comparison. Catalyst activity increases as the particle size decreases at 235 and 250°C, but at 265°C there is no effect of particle size because almost complete CO conversion was obtained with both particle sizes. Particle size has some effect on certain product yields and selectivities as follows. Olefin to paraffin ratios and yield of oxygenates are somewhat higher with smaller particles, whereas other product yields and selectivities do not vary much with the particle size. Trends for C_{12}^{+} products (including wax produced) are rather erratic, and might not be truly representative of the actual steady-state behavior of the system. Comparison of the catalyst performance in the two reactor systems with different particle sizes reveals the following. The activity in the fixed bed reactor is greater than in the slurry bed reactor. Olefin to paraffin ratios and yield of oxygenates are somewhat greater in the fixed bed reactor than in the slurry reactor, whereas the yield of C_{12}^{+} products is higher in the slurry reactor.

2.3.3 Run FB-01-1547 (170/230 mesh fused iron catalyst)

The purpose of this run was to evaluate the catalyst under conditions employed by workers at Exxon using the same particle size and nearly identical reduction procedure. Three mass balances were made during this run

and selected results are shown in Table 5.

Initial conditions were 0.79 MPa (100 psig), 234°C, 1.5 Nℓ/g-cat/h and H_2 CO feed ratio of 1:1. The CO conversion of 36% was lower than the 39% conversion obtained by Exxon workers (as reported by Satterfield *et al.* 1985). At the end of the first mass balance period temperature was raised slowly to 248°C, but after about 2 hours at these conditions a "hot spot" of 50°C was discovered near the top of the bed. The reactor was cooled down in about 30 minutes, and then heated slowly to the desired operating temperature. After that no excessive temperature gradients were observed in the reactor. CO conversion at 245°C was 53% which compares favorably with 60% CO conversion obtained by Exxon workers at 248°C. Product selectivity did not change significantly with the increase in temperature. More wax was collected at 245°C than at 234°C, however this was probably due to the fact that the system did not reach steady-state during the first mass balance. After this balance, process conditions were changed to 1.6 MPa (215 psig), 232°C and 0.75 Nℓ/g·cat/h and another mass balance was made at these conditions. CO and (H_2+CO) conversions were 46 and 41%, respectively. These conversions are smaller than those obtained with much larger particles in the previous runs at nearly the same process conditions (see Table 4). This indicates that the catalyst has deactivated during this run. Some liquid products were lost at the end of the last balance and thus the reported product distribution may not be accurate. Results from the run with 60/100 mesh particles (FA-01-1417, balance 2) are also included for comparison with data obtained during the first mass balance in this run. Catalyst activity was lower in the run with 60/100 mesh particles (CO conversion of 27% vs. 36% with 170/230 mesh particles, STY of 0.015

vs. 0.020 with smaller particles) which is as expected. The liquid products from the cold trap were inadvertently lost and thus comparison of product selectivities is not possible.

Liquid products collected in the cold trap (0°C, atmospheric pressure) follow the ASF distribution, as shown in Fig. 5 for the first mass balance period. Similar results were obtained for the other two mass balances. Negative deviations from the ASF distribution were observed for products with carbon number greater than 16, because these products are mainly present in the heavy fraction collected in a high temperature/high pressure product trap. Products collected in this trap were not quantified.

Selected results obtained in our study, by workers at Exxon, and at MIT (slurry reactor) under similar process conditions are summarized in Table 6. In the slurry bed experiments conducted at MIT (Huff, 1982) an H_2/CO feed ratio of 0.9 was employed, whereas in the fixed bed experiments, conducted in our laboratory and at Exxon, the feed ratio of 1:1 was used. Other conditions are shown in Table 6.

Catalyst activity, measured in terms of CO and (H_2+CO) conversions, was similar in all three studies (the highest activity was obtained in Exxon's study in the fixed bed, whereas the lowest activity was obtained in MIT's study in the slurry reactor). Detailed information on product yields and selectivities was not given for fixed bed experiments conducted at Exxon, and thus direct comparison is possible only for olefin to paraffin ratios at certain carbon numbers. Olefin to paraffin ratios in Exxon's study are much lower than those obtained in our study at both temperatures. Values obtained in our study in the fixed bed reactor are similar to those

obtained at MIT in the slurry reactor. Yields of low molecular weight hydrocarbons (up to C_{11}) are similar in both reactor systems. From these results, as well as those presented earlier in Table 4, it appears that the reactor type does not have significant effect on product selectivity.

2.3.4 Run FA-02-1687 (170/230 mesh, 100Fe/1 Cu/0.2K precipitated catalyst)

This was the first run with a precipitated iron catalyst (uncalcined sample) synthesized in our laboratory and reduced according to the procedure described in Appendix I. The bulk density (1.25 g/cm^3) of this catalyst is much lower than that of fused iron catalyst (2.6 g/cm^3) and thus the bed dilution with inert glass beads was only 2:1 by volume in this run. Four mass balances were made during the run and selected results are given in Table 7.

The first mass balance was made after 27 hours on stream at 1.6 MPa, 2.5 $N\ell/g\cdot cat/h$, 235°C and H_2/CO feed ratio of 1:1. A "hot spot" at 253°C was observed in the uppermost part of the catalyst bed, whereas the bed temperature measured by the other three thermocouples was ~235°C. This occurred after approximately 24 hours on stream and persisted throughout the entire mass balance. As a result of the hot spot, relatively high (H_2+CO) and CO conversions were obtained, 48 and 51% respectively. A space-time-yield of 0.054 mols syngas converted per gram of catalyst per hour was obtained, which is more than twice the value obtained in the run with the fused iron catalyst (FA-1417-1, period 1) at a lower space velocity. Following this, the space velocity was decreased to 1.9 $N\ell/g\cdot cat/h$ (balance 2) and 1.3 $N\ell/g\cdot cat/h$ (balance 3) but in both cases conversions and the space-time-yield were lower than in the first mass balance indicating that the catalyst had deactivated. The temperature was then

raised to 250°C (balance 4) but the conversion continued to decrease (CO: 12%, (H_2+CO) : 12%) and the run was terminated. The "hot spot" was not observed during the last three balances and the bed was nearly isothermal, but apparently the catalyst had deactivated after the first mass balance. Product selectivity in this run was significantly different than that obtained in previous runs with the fused iron catalyst. This catalyst produced more heavy molecular weight products. The selectivity of hydrocarbons during the mass balances 1 and 3 (the loss of liquid products due to a leaky valve occurred during the second mass balance) was: C_1: 3-4.5%; C_2-C_4: 14-20%; C_5-C_{11}: 19-23%, C_{12}^+: 52-64%, whereas in the run FA-01-1417-1 (60/100 mesh fused iron catalyst) it was: C_1: 6%, C_2-C_4: 26%; C_5-C_{11}: 31% and C_{12}^+: 37%.

The ASF plots for the mass balances 1, 3 and 4 are shown in Figures 6-8. Negative deviations from the ASF distribution were obtained in the range C_6-C_9, which is due to partial loss of these products due to volatilization, and beyond C_{14}-C_{16} (mass balances 1 and 3). The latter is due to the fact that products from the high temperature/high pressure trap were not analyzed. Products collected in the cold trap during the last mass balance period (deactivated catalyst) show significant positive deviations from the ASF distribution in the C_{10}-C_{19} range, followed by the usual tailing of at higher carbon numbers.

We plan to make another run with this catalyst during the next month. A new reactor with a volume of 25 cm^3 will be made, so that higher bed dilution ratios can be used, which should help prevent the formation of "hot spots" in the reactor.

2.4 Catalyst Preparation and Characterization

During the past quarter, we have completed the synthesis of all unsupported, precipitated iron catalysts that will be investigated during this project. We have also continued our program of catalyst characterization, including surface area and pore volume distribution measurements, temperature-programmed reduction (TPR) studies of the effect of copper and potassium promoters on the dynamics of iron reduction, and application of Fourier Transform Infrared Spectroscopy (FT-IR) of adsorbed species to examine the chemical nature of surface iron entities on these catalysts. Details of research progress in each of these areas are provided in the following sections.

2.4.1 Catalyst Synthesis

Using the continuous co-precipitation method described in the Quarterly Report, February - April, 1987, we have synthesized 100 g of each of the 25 catalyst compositions that are summarized in Table 8. The compositions shown are nominal expected values in each case, based on known Fe^{3+}/Cu^{2+} ratios in the nitrate solutions used for preparation, and on $KHCO_3$ concentrations used for subsequent deposition of potassium promoter by impregnation of the dried precipitates. We are currently beginning a program of detailed analyses of the actual Fe/Cu/K composition of each material, using inductively-coupled plasma (ICP) atomic absorption spectroscopy. Results of these analyses will be provided in the next report in this series. Preliminary thermal decomposition measurements have indicated, however, that the "as prepared" vacuum-dried precipitates do not consist of essentially pure FeOOH (with copper and/or potassium promoters, if added), as originally expected, but of a more complex mixture of FeOOH,

Fe_2O_3, and, possibly, small amounts of Fe_3O_4 as well.

2.4.2 Catalyst Characterizations

Surface Area/Pore Volume. Total surface areas, obtained by application of the BET method to N_2 adsorption at -196°C, have been measured thus far for selected catalyst compositions, before and after calcination, and are included in Table 8. It is clear from these data that increasing copper content results in increasing surface areas of the dried, uncalcined precipitates. The total surface area of the Fe/Cu/K = 100/20/0 catalyst (374 m^2/g), for example, is more than twice that (180 m^2/g) of the pure, unpromoted iron catalyst. Co-precipitation of CuO evidently decreases the crystallite size and/or modifies the structure of the $FeOOH/Fe_2O_3$ precipitate, leading to a more highly porous, higher surface area material than results in the absence of copper. Following calcination for 4 hrs at 300°C, however, surface areas of both the unpromoted and copper-containing catalysts decrease markedly, to 10 m^2/g or less, due to thermally-induced collapse of the pore structure in each case. The surface area of the copper-free, potassium-promoted catalyst is somewhat larger than that of the unpromoted precipitate from which it was prepared. It is not yet clear why impregnation of $FeOOH/Fe_2O_3$ with such a low level of $KHCO_3$ results in a surface area increase.

In addition to yielding surface area data, complete N_2 adsorption/desorption isotherms that are carried out up to a relative pressure (P/P°) of unity also provide information about pore size distributions and total catalyst pore volumes. Figures 9 and 10 contain examples of such complete isotherms for the same sample of unpromoted iron catalyst before and after treatment in H_2 for 3 hrs at 300°C, respectively. Total gaseous N_2 uptake

of 137 STP cm^3/g at P/P°=1 on the unreduced catalyst (Figure 9) corresponds to a total pore volume of 0.21 cm^3/g. This value decreases to ~ 0.02 cm/g (Figure 10) following thermal treatment in H_2 at 300°C. The uncalcined material exhibits pronounced desorption hysteresis. Application of the Kelvin equation to the desorption branch of the isotherm indicates that the pore size distribution of this material is very narrow, with an average pore radius of 20-25 Å. Following H_2 treatment at 300°C, the isotherm displays no desorption hysteresis (Figure 10), and the pore size distribution becomes very broad, with an ill-defined maximum corresponding to an approximate average pore radius in the range 100-200 Å.

Reduction Behaviors. Reduction in H_2 of all of the precipitated $FeOOH/Fe_2O_3$ catalysts occurs in two steps; the first leads to formation of an intermediate Fe_3O_4 phase, while the second involves subsequent reduction of the latter to metallic iron at higher temperatures and/or longer reduction times:

$$3\ Fe_2O_3 + H_2 \rightarrow 2\ Fe_3O_4 + H_2O \quad (1)$$

$$Fe_3O_4 + 4\ H_2 \rightarrow 3\ Fe + 4\ H_2O \quad (2)$$

It should be noted that reaction (2) consumes eight times more H_2 per mole of Fe than reaction (1). Using the temperature-programmed reduction (TPR) technique that has been described previously (Quarterly Report, February - April, 1987), we have investigated the effects of prior calcination and of copper and potassium promoters on this two-step reduction behavior. Unless otherwise indicated, all TPR studies were performed using 10 mg catalyst samples, a 12 cm^3/min flow rate of 5% H_2/N_2 reductant, and a temperature program rate of 20°C/min.

Typical TPR profiles of an unpromoted $FeOOH/Fe_2O_3$ precipitate are shown in Figure 11, for samples without prior calcination (dashed curve) and after prior calcination in air for 4 hrs at 300°C (solid curve). The peak at 320°C in the profile of the uncalcined sample is due to reduction of residual NO_3^- ions that are not removed by the washing step of the catalyst preparation process:

$$3\ Fe(NO_3)_3 + 14\ H_2 \rightarrow Fe_3O_4 + 9\ NO + 14\ H_2O \qquad (3)$$

This reaction consumes 28 times more H_2 per mole of Fe than does reaction (1) above. Hence, even very small amounts of residual NO_3^- give rise to easily detectable TPR peaks; that in Figure 11, for example, corresponds to only ~ 1% residual $Fe(NO_3)_3$ in the $FeOOH/Fe_2O_3$ precipitate. This peak is not present in the TPR profile of the calcined sample, since prior calcination effects thermal decomposition of the nitrate species. The peak at 400°C in both profiles of Figure 11 is due to reaction (1) above; its area is identical in both profiles, as expected. The broad peaks centered at ~ 600°C are due to the second reduction step of reaction (2). Pre-calcination appears to increase the area of the latter peak somewhat, suggesting that reduction to metallic iron may occur more readily or more completely with samples that have been subjected to prior calcination.

The effect of potassium promoter on the reduction behaviors of copper-free, uncalcined and calcined $FeOOH/Fe_2O_3$ are illustrated by the TPR profiles in Figures 12 and 13; here, the curves labelled 0 K are identical to the dashed and solid curves, respectively, in Figure 11. For both types of catalysts, added potassium has virtually no effect on either the position or the area of the TPR peak at 400°C that corresponds to Fe_3O_4

formation. However, increasing levels of potassium cause both a marked broadening and an increase in area of the high-temperature TPR peak at ~ 600°C that is due to formation of zero-valent iron. The reason for this potassium-modified reduction behavior is not yet clear and is under further investigation.

The promotional effect of copper on iron reduction is demonstrated by the TPR profiles in Figures 14 and 15 for uncalcined and calcined samples, respectively. The curves labelled 0 Cu are again identical to the corresponding dashed and solid curves in Figure 11. The peak in both figures at 200-220°C that increases in area with increasing copper content is due to reduction of CuO to metallic copper:

$$CuO + H_2 \rightarrow Cu + H_2O \qquad (4)$$

The resulting reduced, metallic copper aids in adsorption and activation of H_2, thus facilitating subsequent reduction of iron. It is clear that copper promoter has a pronounced effect on both the positions and shapes of the two iron-related TPR peaks in each profile. Although the overall effect is similar in both cases, it is more marked in the case of pre-calcined catalysts (Figure 15). The presence of even 1 part by weight of Cu per 100 parts of Fe causes a decrease of ~ 150° in the position of the TPR peak that appears at 400-410°C for unpromoted catalysts or for those promoted only with potassium. The beneficial effect of added copper increases with increasing copper content up to a level of 3 Cu/100 Fe, after which further additions up to 20 Cu/100 Fe have little additional effect. In the case of the high-temperature TPR peak at ~ 600°C, the effect of copper promoter is to substantially broaden the peak, indicating that the onset of reduction to metallic iron occurs at progressively lower

temperatures with increasing copper content.

The TPR technique can also be used to estimate the activation energies for the two reduction steps shown in reactions (1) and (2). Assuming plug-flow behavior of the reductant stream and that both reduction steps follow first-order kinetics and are not hydrogen-limited at their maximum rates, the following relationship can be derived (Jones and McNicol, 1986):

$$\ln(T_m^2 \bar{C}_m/\beta) = E/RT_m + \ln(E/RA) \qquad (5)$$

where $\bar{C}_m$ is the mean concentration of H_2 reductant at the temperature (T_m) of maximum reduction rate; β is the temperature program rate; E is the activation energy; R is the gas constant, and A is the Arrhenius frequency factor. Since T_m increases with increasing β, the slope of a plot of $\ln(T_m^2/\beta)$ vs. $1/T_m$ will yield the activation energy, E, if a sufficiently wide range of temperature program rates is used. Figure 16 contains two series of TPR profiles for pre-calcined catalysts containing 0 and 3 parts of Cu per 100 parts of Fe, and that were obtained using 6-fold and 20-fold ranges of β, respectively, and a H_2/N_2 flow rate of 60 cm^3/min. The approximate activation energies derived from these data for reactions (1) and (2) are 25 and 16 kcal/mole, respectively, for the unpromoted catalyst and 19 and 15 kcal/mole for the copper-containing material, in agreement with the previously demonstrated promotional effect of copper on iron reduction.

Surface Properties. Fourier Transform Infrared Spectroscopy (FT-IR) has been used to obtain information about the surface properties of the precipitated iron catalysts, by examining the manner in which selected probe molecules, particularly nitric oxide, NO, interact with surface sites

on these materials. The frequency of the infrared-active N-O stretching vibration is dependent upon the oxidation state of the iron site on which the NO is adsorbed, thus enabling chemical information about the surface sites to be obtained. In all cases, 8% by weight of the catalyst sample was homogenized with silica gel diluent and pressed into a self-supporting wafer (~ 10 mg/cm^2) that was contained in a thermostatted quartz cell connected to a conventional vacuum and gas handling system. The cell design permits evacuation and *in situ* treatment of catalyst samples with desired gases at temperatures up to 800°C. All spectra were obtained using a resolution of 4 cm^{-1} and with the sample at ambient temperature; typically, 100 spectra were collected and averaged for each measurement. All samples were pretreated by calcination in 100 torr of O_2 for 1.5 hrs at 500°C, followed by reduction in 100 torr of H_2 for 1.5 hrs and subsequent evacuation to 1×10^{-5} torr at the same temperature and then cooling in vacuum to ambient temperature.

Spectrum (a) in Figure 17 resulted from exposure of an unpromoted iron catalyst to 12 torr of NO. The bands at 1910 and 1875 cm^{-1} and the unresolved shoulder at 1840 cm^{-1} are due to the R, Q, and P branches, respectively, of the N-O stretching vibration of gaseous NO. These bands are entirely removed, as expected, by brief evacuation of the gas-phase NO [spectrum (b)]. The bands at 1810 and 1740 cm^{-1} in spectrum (a) are due to adsorbed NO on distinguishable types of surface iron sites. These features have been variously interpreted by previous investigators (King and Peri, 1983, Rethwisch and Dumesic, 1986; Busca and Lorenzelli, 1981), and some disagreement remains. The bands are most likely due to NO adsorbed on Fe^{2+} and/or Fe^{3+} (1810 cm^{-1}) and reduced Fe^0 (1740 cm^{-1}). Back donation of

electron density from the zero-valent iron sites weaken the N-O bond, resulting in a decrease of the stretching frequency. Both bands persist virtually unchanged after evacuation of the gaseous NO [spectrum (b)]. Addition of 25 torr of O_2 to the sample [spectrum (c)] causes a gradual decrease in intensity of the two bands due to adsorbed NO and a concomitant appearance of a band at 1625 cm^{-1}. The latter is due to the anti-symmetric stretching vibration (ν_3 mode) of adsorbed NO_2, which is generated by oxidation of the adsorbed NO species on both types of iron sites. Re-admission of gaseous NO, following evacuation of the O_2, failed to re-generate the original bands at 1810 and 1740 cm^{-1} (or any other bands), indicating that the sites responsible for the initial adsorption of NO are destroyed by the O_2 treatment. We have not yet determined whether the Fe^{2+} sites indicated by the FT-IR studies of adsorbed NO are due to incomplete reduction of the original sample (prior to admission of NO) or are generated by oxidation of surface Fe^0 sites by the added NO.

A potassiom-promoted iron sample, containing 1 part K per 100 parts Fe, yielded results similar to those of the unpromoted catalyst, as shown by the spectra in Figure 18. Bands due to adsorption of NO on Fe^{2+} and Fe^0 sites are again generated by admission of gaseous NO [spectrum (a)], although both are "red-shifted" (to 1805 and 1725 cm^{-1}, respectively) by the potassium promoter, and the intensity of the latter band is lower than that observed for the unpromoted sample. Evacuation of the gaseous NO [spectrum (b)] has little effect on either band. However, subsequent admission of gaseous O_2 [spectrum (c)] effects much more rapid removal of the two NO bands, and generation of the NO_2 band at 1625 cm^{-1}, than occurs

with the unpromoted sample. Evacuation of the O_2 and re-admission of gaseous NO again failed to regenerate the bands due to adsorbed NO, as shown in spectrum (a) of Figure 19, but subsequent re-evacuation of the gaseous NO resulted in the formation of two intense bands at 1455 cm^{-1} and ~ 1300-1350 cm^{-1} [spectrum (b)]. The latter bands have not yet been fully characterized, but may be due to the ν_3 vibrational mode of a surface NO_3^- species.

During the next quarter, we plan to perform Fe, Cu, and K elemental analyses of each of the 25 prepared catalysts, using atomic adsorption spectroscopy. We will also complete our measurements of the surface areas and pore size distributions of each material, before and after calcination/reduction, and will continue our TPR and FT-IR characterization studies.

TASK 3 - Process Evaluation Research

This task is scheduled to begin December 1, 1987.

TASK 4 - Economic Evaluation

This task is scheduled to begin June 1, 1988.

V. LITERATURE REFERENCES

Bauer, J.V., Brian, B.W., Dyer, P.N. and Pierantozzi, R., Proc. of the DOE Contractors Conference on Indirect Liquefaction, October 12-13, Pittsburgh, Pennsylvania (1983).

Busca, G., and Lorenzelli., J. Catal. 72, 303 (1981).

Egiebor, N.O., and Cooper, W.C., Appl. Catal. 14, 323 (1985).

Huff, G.A., "Fischer-Tropsch Synthesis in a Slurry Reactor," Sc.D. Thesis, M.I.T. (1982).

Huff, G.A. and Satterfield, C.N., J. Catal. 85, 370 (1984).

Jones, A. and McNicol, B., "Temperature-Programmed Reduction for Solid Materials Characterization," Marcel Dekker, N.Y. (1986).

King, D. L. and Peri, J. B., J. Catal. 79, 164 (1983).

Rethwisch, D. G. and Dumesic, J. A., J. Phys. Chem. 90, 1625 (1986).

Satterfield, C.N., Huff, G.A., Stenger, H.G., Carter, J.L., and Madon, R.J., Ind. Eng. Chem. Fundam. 24, 450 (1985).

Table 1. Summary of results for fixed bed, Run FA-01-1537.

Catalyst: 6.60 g (a), UCI C-73-01 Fused Iron Diluent: 15.48 g, Glass beads
Catalyst size: 30/60 mesh Diluent size: 30/60 mesh
Catalyst volume: 2.50 cc Diluent volume: 10.00 cc

Period	1	2	3
Date	06/03/87	06/04/87	06/05/87
Time on stream (h)	20.0	40.5	66.0
Balance duration (h)	6.0	6.0	6.0
Average reactor temp (C)	235.	250.	266.
Max reactor temp gradient (C) (b)	.5	1.7	1.3
Reactor pres (MPa)	1.58	1.58	1.58
H2/CO molar feed ratio	.97	.97	.97
Space velocity (Nl/g-cat*h) (a)	.75	.76	.76
Space velocity (Nl/g-Fe*h) (a)	1.12	1.13	1.14
GHSV (1/h) (c)	1980.	2003.	2015.
Weight closure (%)	93.2	91.5	93.9
H2 conversion (%)	43.8	63.8	74.3
CO conversion (%)	60.4	90.7	97.9
H2+CO conversion (%)	52.2	77.4	86.3
H2/CO molar usage	.705	.684	.738
STY (mols H2+CO/g-cat*h) (a)	.017	.026	.029
Chain growth probability factor (Based on selected points)	.70	.68	.69
[P-CO2][P-H2]/[P-CO][P-H2O]	8.6	28.9	60.1
Wt % of outlet			
H2	3.94	2.59	1.79
H2O	2.82	3.44	5.38
CO	39.67	9.54	2.08
CO2	42.74	64.44	65.93
Hydrocarbons	9.51	15.72	20.42
Oxygenates	1.25	1.55	1.60
Wax (d)	.07	2.71	2.80
Yield (g/Nm3-syngas converted)			
C1	10.42	16.42	19.20
C2-C4	46.95	54.07	58.91
C5-C11	51.21	51.78	67.20
C12-C17	6.45	3.72	5.38
C18+ (e)	.01	.01	.00
Oxygenates	15.09	12.42	11.82
Wax (d)	.84	21.71	20.67
Total	130.96	160.14	183.18

(a) Based on unreduced catalyst; (b) Maximum axial temperature difference;
(c) Based on catalyst volume; (d) Products collected from hot trap;
(e) Does not include wax

Table 1 (cont'd). Summary of results for fixed bed, Run FA-01-1537.

Period	1	2	3
Wt % of Hydrocarbons			
Methane	8.99	11.11	11.20
Ethane	4.95	5.68	4.96
Ethylene	7.52	5.05	4.56
Propane	2.84	2.56	2.22
Propylene	12.26	11.70	11.56
n-Butane	2.60	2.14	1.81
1+2 Butenes	9.24	8.54	8.38
C4 Isomers	1.10	.93	.88
n-Pentane	2.96	2.41	2.12
1+2 Pentenes	7.52	6.68	6.64
C5 Isomers	.83	.73	.72
n-Hexane	.08	.20	.30
1+2 Hexenes	6.57	5.34	4.95
C6 Isomers	1.26	.91	.84
n-Heptane	.23	.42	.61
1+2 Heptenes	3.79	3.41	3.71
C7 Isomers	.62	.39	.38
n-Octane	.76	.86	1.26
1+2 Octenes	3.23	2.83	4.02
C8 Isomers	.16	.28	.35
n-Nonane	1.45	1.04	1.39
1+2 Nonenes	3.85	2.72	3.89
C9 Isomers	.16	.53	.46
n-Decane	1.43	.90	1.13
1+2 Decenes	3.87	2.24	3.01
C10 Isomers	.68	.55	.39
n-Undecane	1.10	.66	.82
1+2 Undecenes	3.05	1.55	2.03
C11 Isomers	.59	.40	.20
C2+ (e)	90.29	74.19	76.73
C2-C4	40.52	36.60	34.38
C5-C11	44.20	35.06	39.22
C12-C17	5.56	2.52	3.14
C18+ (e)	.01	.01	.00
Wax (d)	.72	14.70	12.06

(d) Products collected from hot trap; (e) Does not include wax

Table 2. Effect of catalyst reduction procedure.

P = 1.58 MPa
SV = 0.75 Nℓ/g-cat·h
$(H_2/CO)_{feed}$ = 1.0
Particle mesh size = 30/60

Temperature (°C)	235		250		266	
Run number	1147-2	1537-1	1147-3	1537-2	1147-1	1537-3
H_2 + CO conversion	32.1	52.2	53.2	77.4	70.4	86.3
CO conversion	29.8	60.4	58.7	90.7	79.1	97.9
H_2/CO usage	1.1	0.7	0.8	0.7	0.8	0.7
STY (mol H_2 + CO/g-cat·h)	.011	.017	.018	.026	.023	.029
Olefin/Paraffin ratio						
C_2	1.3	1.6	1.4	1.0	1.0	1.0
C_3	2.9	4.5	3.6	4.8	4.2	5.5
C_4	3.4	3.7	3.9	4.1	4.2	4.8
C_8	6.0	4.3	3.9	3.3	3.6	3.2
C_{10}	2.9	2.7	3.0	2.5	3.0	2.7
Yield (g/Nm^3 H_2 + CO converted)						
CH_4	12.1	10.4	15.8	16.4	17.0	19.2
C_2-C_4	49.2	47.0	34.6	54.1	48.6	58.9
C_5-C_{11}	43.2	51.2	32.3	51.8	49.4	67.2
C_{12}^+, including wax	101	7.3	73.5	25.5	23.2	26.1
Oxygenates	4.0	15.1	8.5	12.4	8.5	11.8
CO_2	429	517	530	516	510	487

Table 3. Summary of results for fixed bed, Run FA-01-1417.

Catalyst: 5.00 g (a), UCI C-73-01 Fused Iron Diluent: 15.10 g, Glass beads
Catalyst Size: 60/100 mesh Diluent Size: 60/100 mesh
Catalyst volume: 2.51 cc Diluent volume: 10.00 cc

Period	1	3	4	5	6
Date	05/23/87	5/25/87	5/26/87	5/26/87	05/28/87
Time on stream (h)	39.5	88.0	112.2	135.2	159.0
Balance duration (h)	6.0	6.5	6.3	6.0	6.0
Average reactor temp (C)	235.	250.	265.	250.	236.
Max reactor temp gradient (C) (b)	2.6	3.9	5.1	3.2	2.0
Reactor pres (MPa)	1.64	1.57	1.62	1.58	1.58
H2/CO molar feed ratio	.97	.97	.97	.97	.97
Space velocity (Nl/g-cat*h) (a)	.74	.75	.76	.76	.75
Space velocity (Nl/g-Fe*h) (a)	1.11	1.13	1.13	1.13	1.12
GHSV (1/h) (c)	1480.	1502.	1510.	1510.	1498.
Weight closure (%)	96.5	91.0	95.3	89.8	97.5
H2 conversion (%)	61.9	71.1	74.0	55.3	30.7
CO conversion (%)	83.9	97.2	98.1	80.9	46.8
H2+CO conversion (%)	73.1	84.3	86.2	68.3	38.9
H2/CO molar usage	.718	.711	.733	.665	.639
STY (mols H2+CO/g-cat*h) (a)	.024	.028	.029	.023	.013
Chain growth probability factor (Based on selected points)	.74/.87(g)	.72	.67	.69	.72
[P-CO2][P-H2]/[P-CO][P-H2O]	8.2	6554.3(f)	70.6	18.9	7.5
Wt % of outlet					
H2	2.58	2.08	1.79	3.25	4.65
H2O	6.44	.04 (f)	5.44	2.86	2.25
CO	15.60	2.88	1.83	19.83	51.00
CO2	55.95	70.04	69.09	57.84	32.48
Hydrocarbons	16.25	18.63	18.90	13.55	7.81
Oxygenates	2.08	2.38	1.82	1.63	1.27
Wax (d)	1.10	3.96	1.14	1.03	.55
Yield (g/Nm3-syngas converted)					
C1	9.76	16.24	18.39	15.39	8.32
C2-C4	41.32	51.84	58.92	50.54	50.24
C5-C11	48.33	63.38	60.38	47.64	59.15
C12-C17	24.28	4.78	3.90	7.22	15.06
C18+ (e)	21.84	.01	.00	.00	.03
Oxygenates	18.62	17.37	13.67	14.56	21.58
Wax (d)	9.83	28.99	8.55	9.21	9.35
Total	173.97	182.60	163.81	144.55	163.73

(a) Based on unreduced catalyst; (b) Maximum axial temperature difference;
(c) Based on catalyst volume; (d) Products collected from hot trap;
(e) Does not include wax; (f) Aqueous product lost in sample handling;
(g) Values for low and high carbon number ranges

Table 3 (cont'd). Summary of results for fixed bed, Run FA-01-1417.

Period	1	3	4	5	6
Wt % of Hydrocarbons					
Methane	6.28	9.83	12.25	11.84	5.85
Ethane	2.40	3.66	4.70	4.89	4.26
Ethylene	5.33	5.36	6.19	6.53	6.51
Propane	1.65	1.85	2.17	2.59	2.64
Propylene	8.61	10.29	13.37	12.21	10.53
n-Butane	1.62	1.68	1.90	2.22	2.39
1+2 Butenes	6.22	7.60	9.75	9.04	7.99
C4 Isomers	.76	.93	1.16	1.39	1.03
n-Pentane	2.08	2.03	2.50	2.68	2.76
1+2 Pentenes	5.53	6.66	8.01	6.99	6.41
C5 Isomers	.71	.71	.91	.91	.82
n-Hexane	.67	1.09	1.19	.16	1.20
1+2 Hexenes	3.31	3.73	4.93	5.01	4.31
C6 Isomers	.73	.67	1.07	.94	1.01
n-Heptane	.59	.90	1.41	.31	.17
1+2 Heptenes	2.30	3.33	3.24	3.23	3.68
C7 Isomers	.44	.33	.62	.44	.57
n-Octane	.72	1.06	.79	.68	.79
1+2 Octenes	2.47	3.85	3.23	2.78	3.03
C8 Isomers	.20	.36	.84	.36	.21
n-Nonane	.92	1.16	.89	.93	1.31
1+2 Nonenes	2.85	3.88	3.13	2.81	3.17
C9 Isomers	.11	.64	.65	.73	.44
n-Decane	.91	.92	.73	.83	1.43
1+2 Decenes	2.89	3.15	2.55	2.59	3.74
C10 Isomers	.12	.69	.72	.85	.95
n-Undecane	.84	.62	.53	.67	1.26
1+2 Undecenes	2.64	2.17	1.77	2.10	3.53
C11 Isomers	.07	.44	.52	.68	.84
C2+ (e)	87.39	72.63	82.06	81.08	87.57
C2-C4	26.60	31.37	39.24	38.88	35.34
C5-C11	31.11	38.36	40.21	36.65	41.61
C12-C17	15.63	2.89	2.60	5.55	10.59
C18+ (e)	14.06	.00	.00	.00	.02
Wax (d)	6.33	17.54	5.70	7.08	6.58

(d) Products collected from hot trap; (e) Does not include wax

Table 4. Effect of catalyst particle size and comparison of fixed bed and slurry bed performance.

P = 1.48 - 1.64 $(H_2/CO)_{feed}$ = 1.0

SY = 0.70 - 0.76 NM/g-cat·h

Temperature (°C)	235			250			265		
Reactor	Fixed	Bed	Slurry	Fixed	Bed	Slurry	Fixed	Bed	Slurry
Run number	1537-1	1417-1	0817-3	1537-2	1417-3	0817-4	1537-3	1417-4	0817-5
Particle mesh size	30/60	60/100	<325	30/60	60/100	<325	30/60	60/100	<325
H_2 + CO conversion	52.2	73.1	38.7	77.4	84.3	72.6	86.3	86.2	77.9
CO conversion	60.4	83.9	50.5	90.7	97.2	87.5	97.9	98.1	93.5
H_2/CO usage	0.7	0.7	0.6	0.7	0.7	0.7	0.7	0.7	0.7
STY (mol H_2 + CO/g-cat·h)	.017	.024	.012	.026	.028	.024	.029	.029	.026
Olefin/Paraffin ratio									
C_2	1.6	2.4	1.9	1.0	1.6	0.5	1.0	1.4	0.6
C_3	4.5	5.1	3.4	4.8	5.8	3.3	5.5	6.5	6.9
C_4	3.7	4.0	2.7	4.1	4.7	2.9	4.8	5.3	4.1
C_8	4.3	3.1	2.4	3.3	3.5	1.5	3.2	4.0	2.2
C_{10}	2.7	3.2	1.7	2.5	3.4	1.1	2.7	3.5	2.2
Yield (g/Nm^3 H_2 + CO converted)									
CH_4	10.4	9.7	27.9	16.4	16.2	22.1	19.2	18.3	24.2
C_2-C_4	47.0	40.2	44.5	54.1	51.6	47.5	58.9	58.6	57.9
C_5-C_{11}	51.2	44.9	39.4	51.8	62.9	44.8	67.2	59.9	46.2
C_{12}^+, including wax	7.3	51.0	98.1	25.5	33.8	87.8	26.1	12.5	35.0
Oxygenates	15.1	15.2	18.3	12.4	17.6	5.1	11.8	13.8	3.9
CO_2	517	498	573	516	509	553	487	515	548

Table 5. Summary of results for fixed bed, Run FB-01-1547.

Catalyst: 7.81 g (a), UCI C-73-01 Fused Iron Diluent: 17.80 g, Glass beads
Catalyst size: 170/230 mesh Diluent size: 170/230 mesh
Catalyst volume: 3.00 cc Diluent volume: 12.00 cc

Run	FB-01-1547			FA-01-1417 (g)
Period	1	2	3	2
Date	6/04/87	6/05/87	06/07/87	05/24/87
Time on stream (h)	18.0	46.0	90.2	64.5
Balance duration (h)	6.0	8.5	6.0	7.0
Average reactor temp (C)	234.	245.	235.	233
Max reactor temp gradient (C) (b)	4.0	6.0	4.0	.6
Reactor pres (MPa)	.83	.83	1.60	.79
H2/CO molar feed ratio	.97	.97	.97	.97
Space velocity (Nl/g-cat*h) (a)	1.51	1.47	.75	1.52
Space velocity (Nl/g-Fe*h) (a)	2.25	2.20	1.11	2.26
GHSV (1/h) (c)	3924.	3833.	1942.	3022
Weight closure (%)	93.2	94.8	90.6	95.9
H2 conversion (%)	23.7	32.5	35.3	16.4
CO conversion (%)	35.9	53.1	45.8	27.0
H2+CO conversion (%)	29.9	42.9	40.6	21.8
H2/CO molar usage	.643	.595	.749	.591
STY (mols H2+CO/g-cat*h) (a)	.020	.028	.014	.015
Chain growth probability factor (Based on selected points)	.67	.69	.71	.71
[P-CO2][P-H2]/[P-CO][P-H2O]	5.7	12.7	186.8 (f)	4.6
Wt % of outlet				
H2	5.35	4.66	4.67	5.70
H2O	1.78	1.62	.07 (f)	1.50
CO	64.32	46.27	55.89	71.16
CO2	21.54	35.98	28.68	15.18
Hydrocarbons	5.94	8.70	8.59	4.66
Oxygenates	.63	.90	.29	.51
Wax (d)	.44	1.86	1.81	1.29
Yield (g/Nm3-syngas converted)				
C1	12.82	10.04	8.06	(h)
C2-C4	51.62	54.92	56.00	—
C5-C11	53.69	55.77	52.03	—
C12-C17	7.31	9.52	13.89	—
C18+ (e)	.10	.02	.01	—
Oxygenates	13.32	13.53	4.42	—
Wax (d)	9.33	27.86	27.34	—
Total	148.19	171.67	161.74	—

(a) Based on unreduced catalyst; (b) Maximum axial temperature difference;
(c) Based on catalyst volume; (d) Products collected from hot trap;
(e) Does not include wax; (f) Aqueous product lost in sample handling;
(g) 60/100 mesh catalyst; (h) Liquid product lost in sample handling

Table 5 (cont'd). Summary of results for fixed bed, Run FB-01-1547.

Period	1	2	3	2
Wt % of Hydrocarbons				
Methane	9.51	6.35	5.12	(h)
Ethane	2.44	4.18	4.98	—
Ethylene	9.57	7.12	6.52	—
Propane	2.14	1.85	2.51	—
Propylene	11.77	10.87	10.39	—
n-Butane	2.15	1.70	2.24	—
1+2 Butenes	9.16	8.11	7.75	—
C4 Isomers	1.03	.90	1.20	—
n-Pentane	2.82	2.19	2.51	—
1+2 Pentenes	8.07	7.30	7.07	—
C5 Isomers	.78	.87	1.06	—
n-Hexane	.02	.03	1.26	—
1+2 Hexenes	7.55	5.90	4.24	—
C6 Isomers	1.38	1.16	1.02	—
n-Heptane	.04	.10	.00	—
1+2 Heptenes	4.65	3.96	3.05	—
C7 Isomers	.77	.78	.40	—
n-Octane	.30	.45	.04	—
1+2 Octenes	2.81	2.60	1.78	—
C8 Isomers	.35	.47	.28	—
n-Nonane	.67	.75	.41	—
1+2 Nonenes	2.20	1.80	1.43	—
C9 Isomers	.05	.25	.00	—
n-Decane	.79	.81	.89	—
1+2 Decenes	2.70	2.13	2.90	—
C10 Isomers	.19	.54	.04	—
n-Undecane	.68	.72	1.08	—
1+2 Undecenes	2.50	2.00	3.42	—
C11 Isomers	.50	.47	.20	—
C2+ (e)	83.57	76.03	77.50	—
C2-C4	38.27	34.73	35.60	—
C5-C11	39.80	35.27	33.07	—
C12-C17	5.42	6.02	8.83	—
C18+ (e)	.08	.01	.01	—
Wax (d)	6.92	17.62	17.38	—

(d) Products collected from hot trap; (e) Does not include wax;
(h) Liquid product lost in sampling handling

Table 6. Comparison with literature for fixed bed and slurry bed performance.

P = 0.79 - 0.83 MPa
SV = 1.5 NM/g-cat·h
$(H_2/CO)_{feed}$ = 0.9 - 1.0

Temperature (°C)	232-235			245-248		
Reactor	Fixed Bed		Slurry	Fixed Bed		Slurry
Run number	1547-1	Exxon 746[1]	MIT 9-16[1,2]	1547-2	Exxon 652[1]	MIT 9-4[1,2]
Particle mesh size	170/230	170/230	<325	170/230	170/230	<325
H_2 + CO conversion	29.9	NR	26	42.9	NR	46
CO conversion	35.9	49	29	53.1	60	54
H_2/CO usage	0.6	NR	0.7	0.6	NR	0.6
STY (mol H_2 + CO/g-cat·h)	.020	NR	.018	.028	NR	.032
Olefin/Paraffin ratio						
C_2	4.2	.15	4.6	1.8	0.1	3.7
C_3	5.8	0.8	4.9	6.2	0.4	5.6
C_4	4.4	0.9	4.0	4.9	1.2	4.5
C_8	3.7	NR	2.7	3.0	NR	2.9
C_{10}	3.4	NR	2.4	2.7	1.2	3.2
Yield (g/Nm^3 H_2 + CO converted)						
CH_4	12.1	NR	11.9	10.0	NR	15.6
C_2-C_4	50.5	NR	46.6	54.9	NR	53.4
C_5-C_{11}	52.8	NR	54.5	55.8	NR	55.4
C_{12}^+, including wax	16.7	NR	76.7	37.4	NR	17.4
Oxygenates	13.3	NR	20.2	13.5	NR	23.6
CO_2	440	NR	555	539	NR	577

(1) Exxon data from Satterfield et al. (1985).

(2) Data from Huff (1982).

NR = Not Reported.

Table 7. Summary of results for fixed bed, Run FA-02-1687.

Catalyst: 5.00 g (a), 100Fe/1Cu/0.2K
Catalyst size: 170/230 mesh
Catalyst volume: 4.00 cc

Diluent: 12.55 g, Glass beads
Diluent size: 170/230 mesh
Diluent volume: 8.00 cc

Period	1	2	3	4
Date	06/18/87	06/19/87	06/20/87	06/21/87
Time on stream (h)	27.0	50.5	73.0	96.5
Balance duration (h)	6.0	6.0	6.0	7.5
Average reactor temp (C)	235.	236	235.	250.
Max reactor temp gradient (C) (b)	18.0	4.3	1.6	.9
Reactor pres (MPa)	1.48	1.48	1.48	1.48
H2/CO molar feed ratio	.97	0.97	1.05	1.05
Space velocity (Nl/g-cat*h) (a)	2.51	1.87	1.26	1.27
Space velocity (Nl/g-Fe*h) (a)	4.04	3.02	2.03	2.04
GHSV (1/h) (c)	3140.	2342.	1573.	1582.
Weight closure (%)	96.4	88.5(f)	96.1	99.2
H2 conversion (%)	46.3	35.8	34.0	12.2
CO conversion (%)	50.7	38.4	42.2	12.3
H2+CO conversion (%)	48.5	37.2	38.0	12.2
H2/CO molar usage	.888	.910	.845	1.037
STY (mols H2+CO/g-cat*h) (a)	.054	.030	.021	.007
Chain growth probability factor (Based on selected points)	.78	(f)	.74	.63/.91(g)
[P-CO2][P-H2]/[P-CO][P-H2O]	2.1	(f)	1.8	1.2
Wt % of outlet				
H2	3.64	(f)	4.83	6.22
H2O	5.71	—	6.15	1.94
CO	47.79	—	55.92	82.21
CO2	27.92	—	22.38	5.56
Hydrocarbons	6.11	—	5.51	2.29
Oxygenates	.70	—	.92	.39
Wax (d)	8.13	—	4.29	1.39
Yield (g/Nm3-syngas converted)				
C1	6.25	(f)	7.40	17.96
C2-C4	27.16	—	32.25	39.19
C5-C11	35.88	—	37.30	37.79
C12-C17	13.08	—	14.28	25.74
C18+ (e)	.01	—	.06	1.37
Oxygenates	9.46	—	15.32	20.93
Wax (d)	109.49	—	71.14	73.75
Total	201.32	—	177.76	216.74

(a) Based on unreduced catalyst; (b) Maximum axial temperature difference;
(c) Based on catalyst volume; (d) Products collected from hot trap;
(e) Does not include wax; (f) Aqueous, organic product lost in sample handling;
(g) Values for low and high carbon number ranges

Table 7 (cont'd). Summary of results for fixed bed, Run FA-02-1687.

Period	1	2	3	4
Wt % of Hydrocarbons				
Methane	3.26	(f)	4.55	9.17
Ethane	.89	—	1.61	3.35
Ethylene	3.30	—	4.49	4.25
Propane	.72	—	1.10	1.55
Propylene	4.43	—	6.14	5.03
n-Butane	.72	—	1.02	1.23
1+2 Butenes	3.69	—	4.91	4.07
C4 Isomers	.41	—	.57	.54
n-Pentane	.90	—	1.23	1.21
1+2 Pentenes	3.19	—	4.36	4.63
C5 Isomers	.30	—	.48	.54
n-Hexane	.00	—	.10	.00
1+2 Hexenes	2.17	—	2.37	3.85
C6 Isomers	.37	—	.47	.67
n-Heptane	.01	—	.00	.02
1+2 Heptenes	1.44	—	1.65	2.95
C7 Isomers	.22	—	.22	.46
n-Octane	.11	—	.18	.03
1+2 Octenes	1.40	—	1.43	1.49
C8 Isomers	.11	—	.04	.05
n-Nonane	.36	—	.53	.14
1+2 Nonenes	1.84	—	2.08	.38
C9 Isomers	.02	—	.04	.01
n-Decane	.52	—	.75	.29
1+2 Decenes	2.41	—	2.78	.77
C10 Isomers	.08	—	.23	.03
n-Undecane	.57	—	.81	.45
1+2 Undecenes	2.55	—	2.91	1.21
C11 Isomers	.15	—	.31	.12
C2+ (e)	39.68	—	51.65	53.16
C2-C4	14.15	—	19.85	20.02
C5-C11	18.70	—	22.96	19.30
C12-C17	6.82	—	8.79	13.15
C18+ (e)	.00	—	.04	.70
Wax (d)	57.06	—	43.80	37.67

(d) Products collected from hot trap; (e) Does not include wax;
(f) Aqueous, organic product lost in sample handling

Table 8. Compositions and surface areas of synthesized precipitated iron catalysts.

Nominal Composition (parts by weight)			Surface Area (m^2/g)	
Fe	Cu	K	Uncalcined	Calcined*
100	0.0	0.00	180	10
	0.0	0.01		
		0.02		
		0.05		
		0.10		
		0.20		
		0.50		
		1.00	210	
		2.00		
	0.1	0.00		
	0.3	0.00		
		0.05		
		0.20		
		0.50		
	1.0	0.00	195	
		0.05		
		0.20		
		0.50		
	3.0	0.00	300	
		0.05		
		0.20		
		0.50		
	10.0	0.00		
	20.0	0.00	374	8
	22.0	0.60		

* 4 hrs at 300°C.

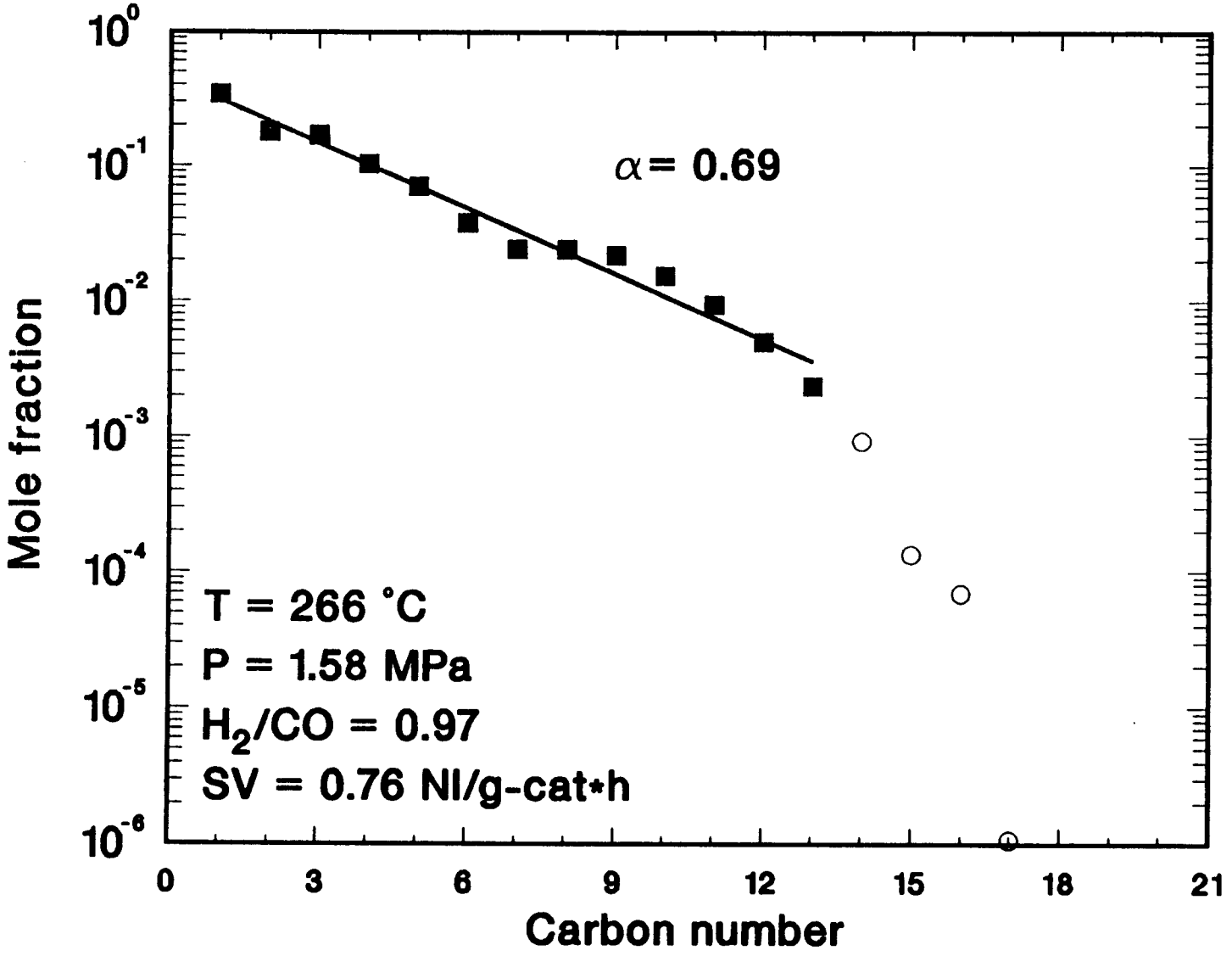

Figure 1. Anderson-Schulz-Flory plot for run FA-01-1537-3.

(The entire product spectrum was not analyzed)

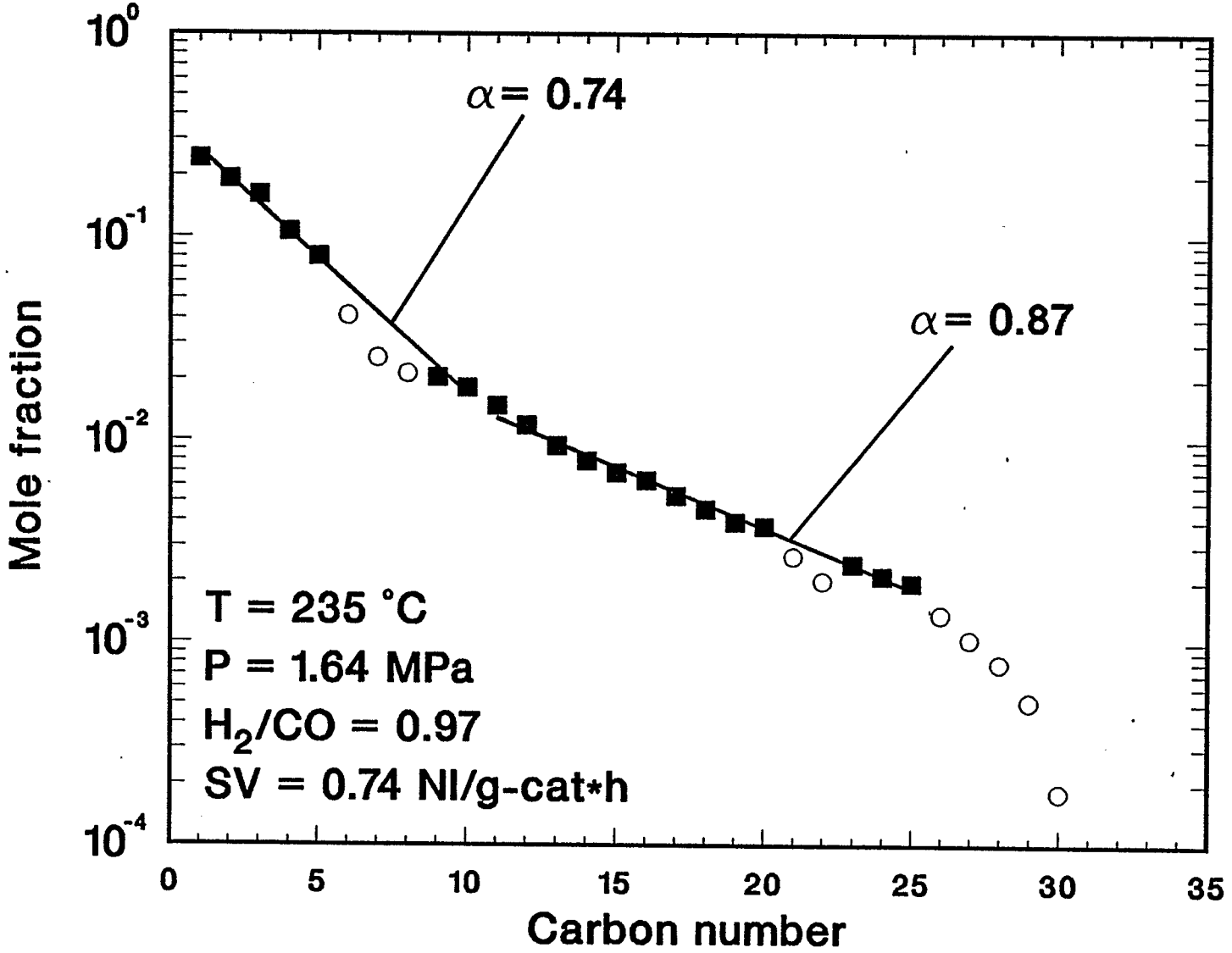

Figure 2. Anderson-Schulz-Flory plot for run FA-01-1417-1.

(The entire product spectrum was not analyzed)

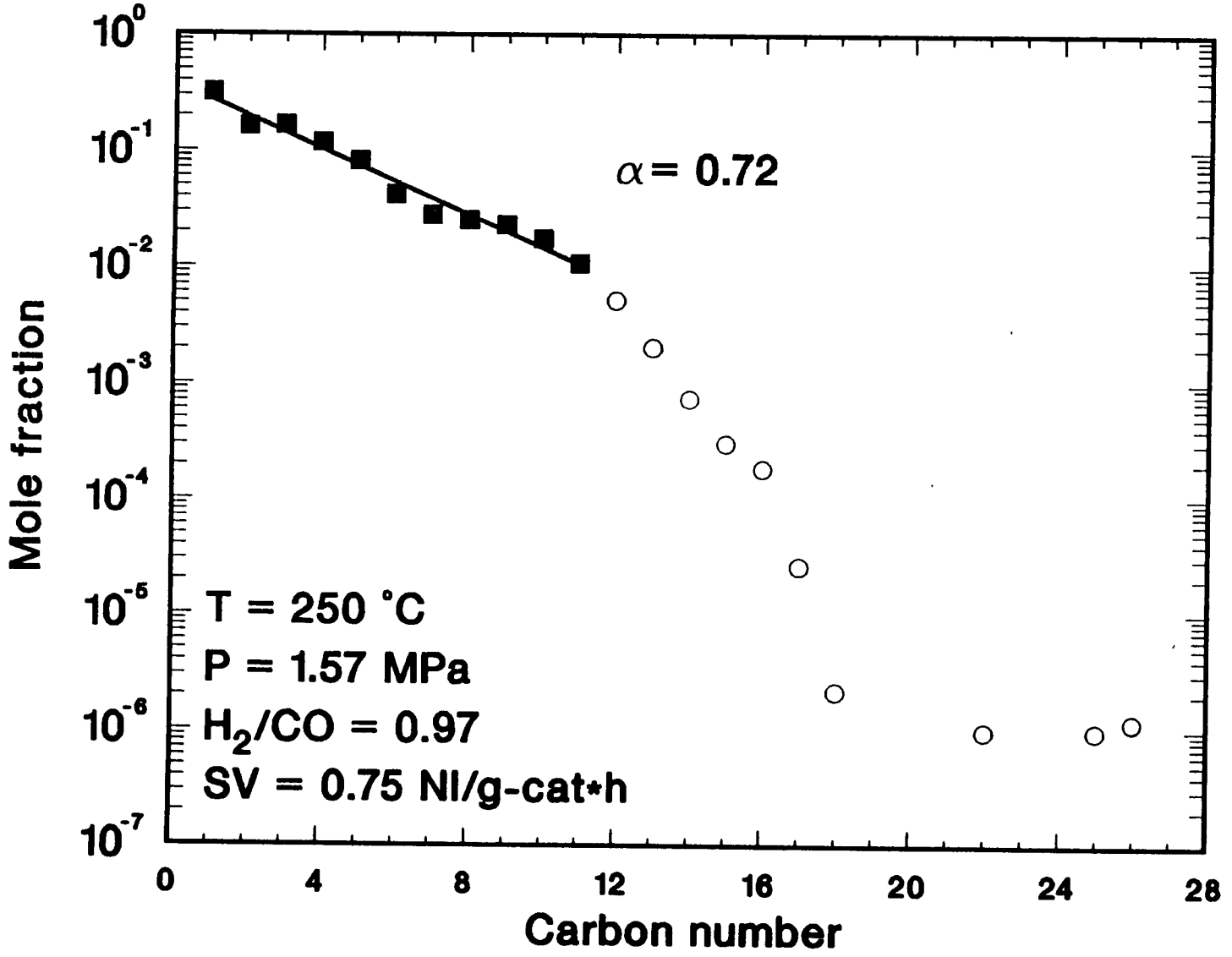

Figure 3. Anderson-Schulz-Flory plot for run FA-01-1417-3.

(The entire product spectrum was not analyzed)

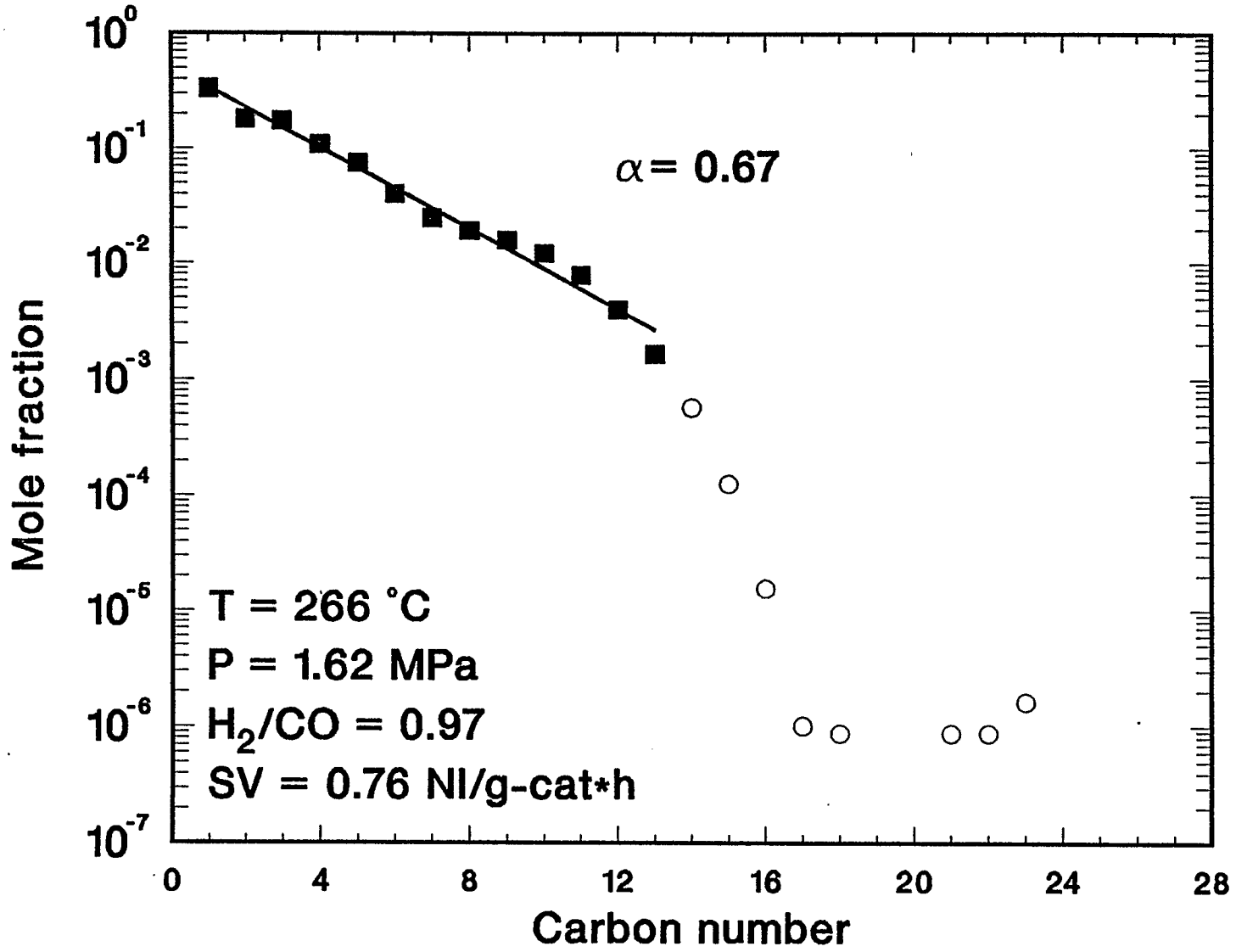

Figure 4. Anderson-Schulz-Flory plot for run FA-01-1417-4.

(The entire product spectrum was not analyzed)

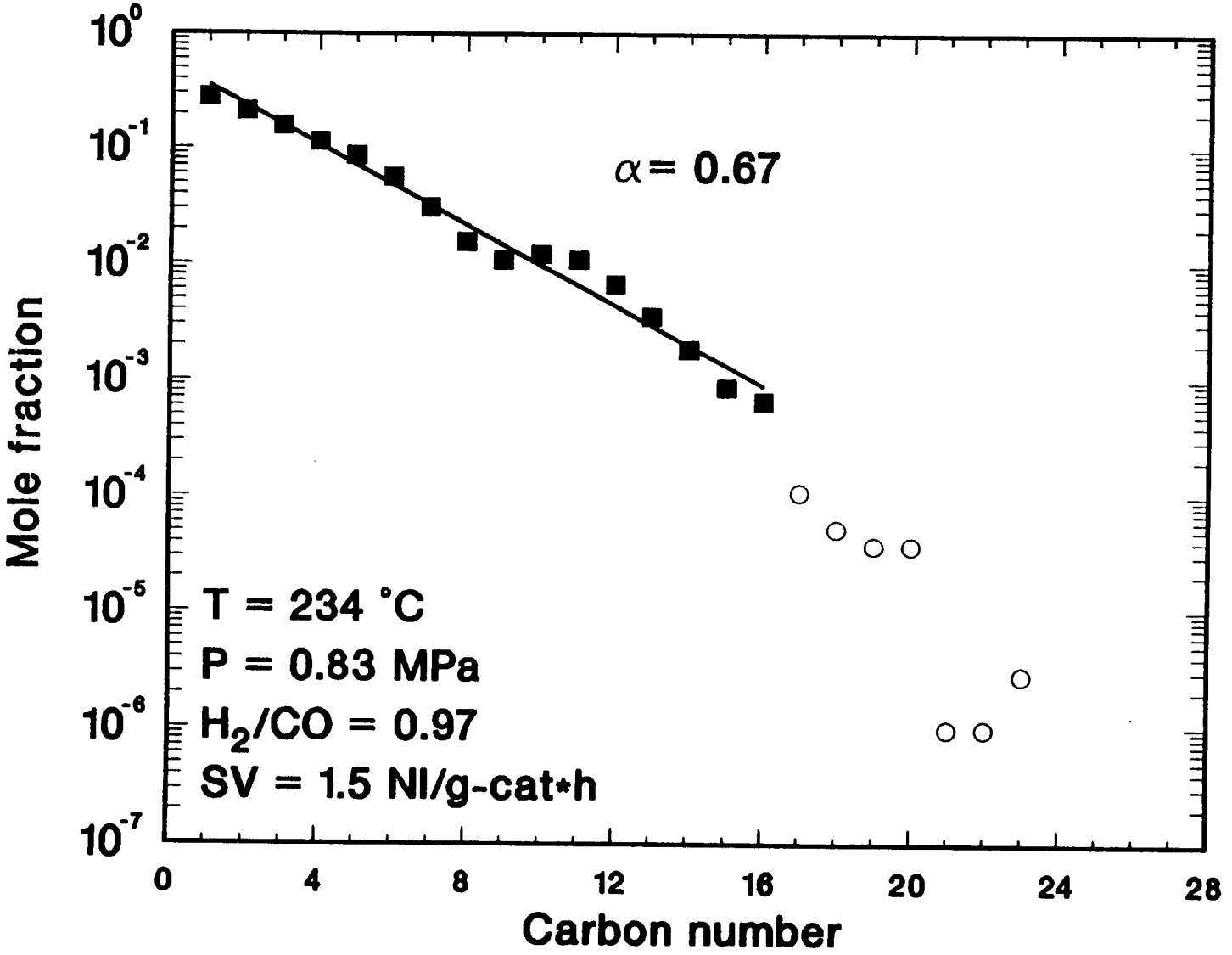

Figure 5. Anderson-Schulz-Flory plot for run FA-01-1547-1.

(The entire product spectrum was not analyzed)

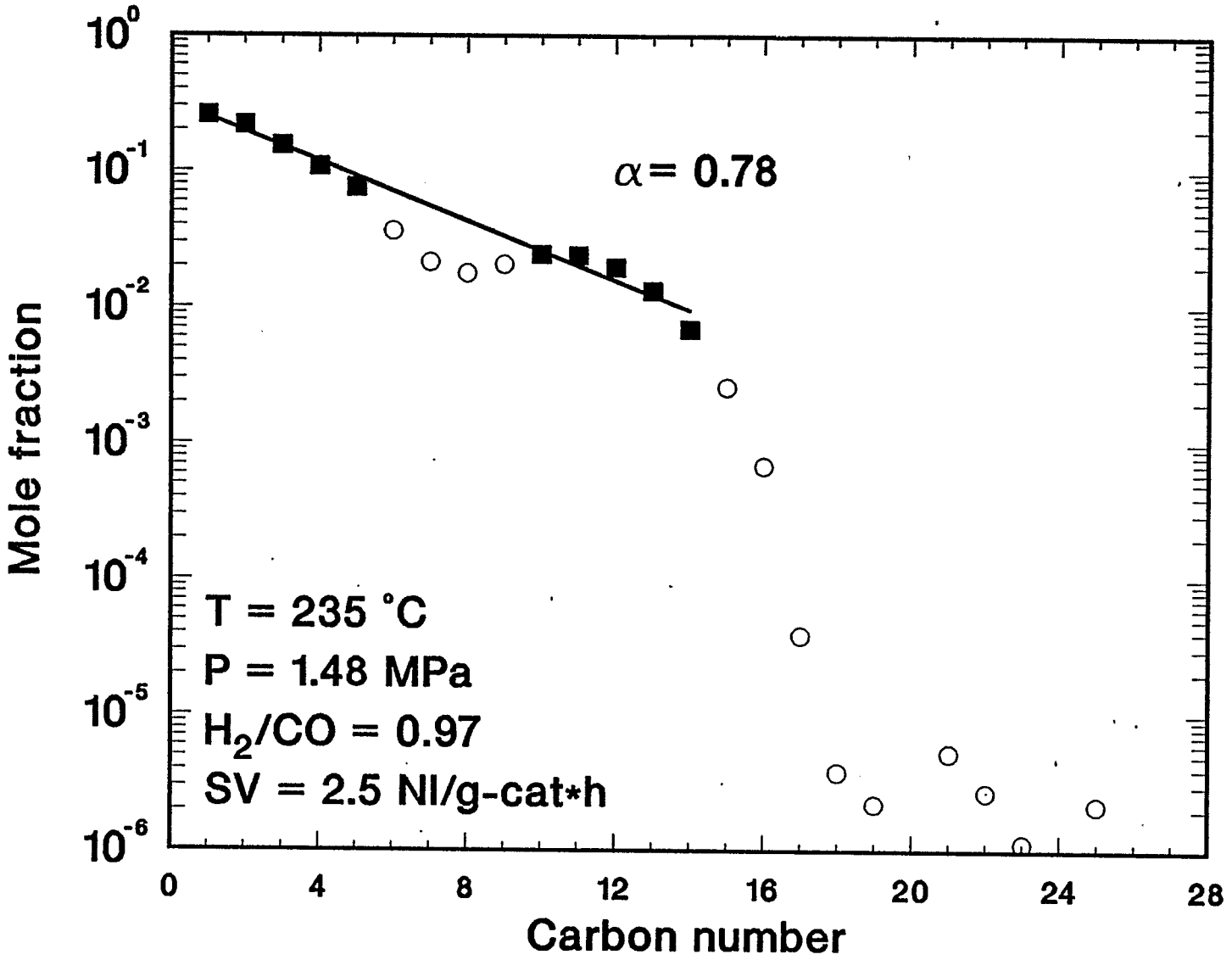

Figure 6. Anderson-Schulz-Flory plot for run FA-01-1687-1.

(The entire product spectrum was not analyzed)

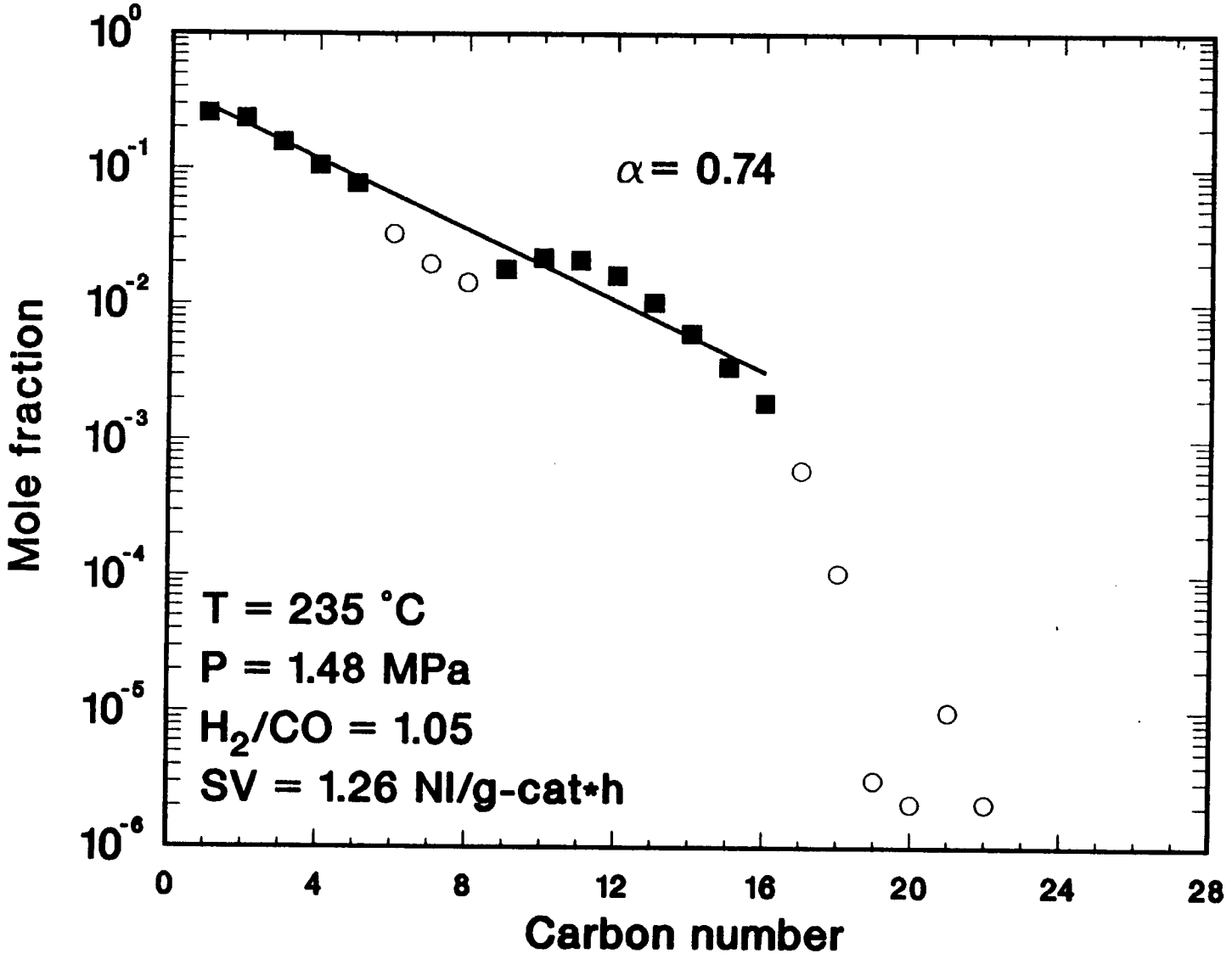

Figure 7. Anderson-Schulz-Flory plot for run FA-01-1687-3.

(The entire product spectrum was not analyzed)

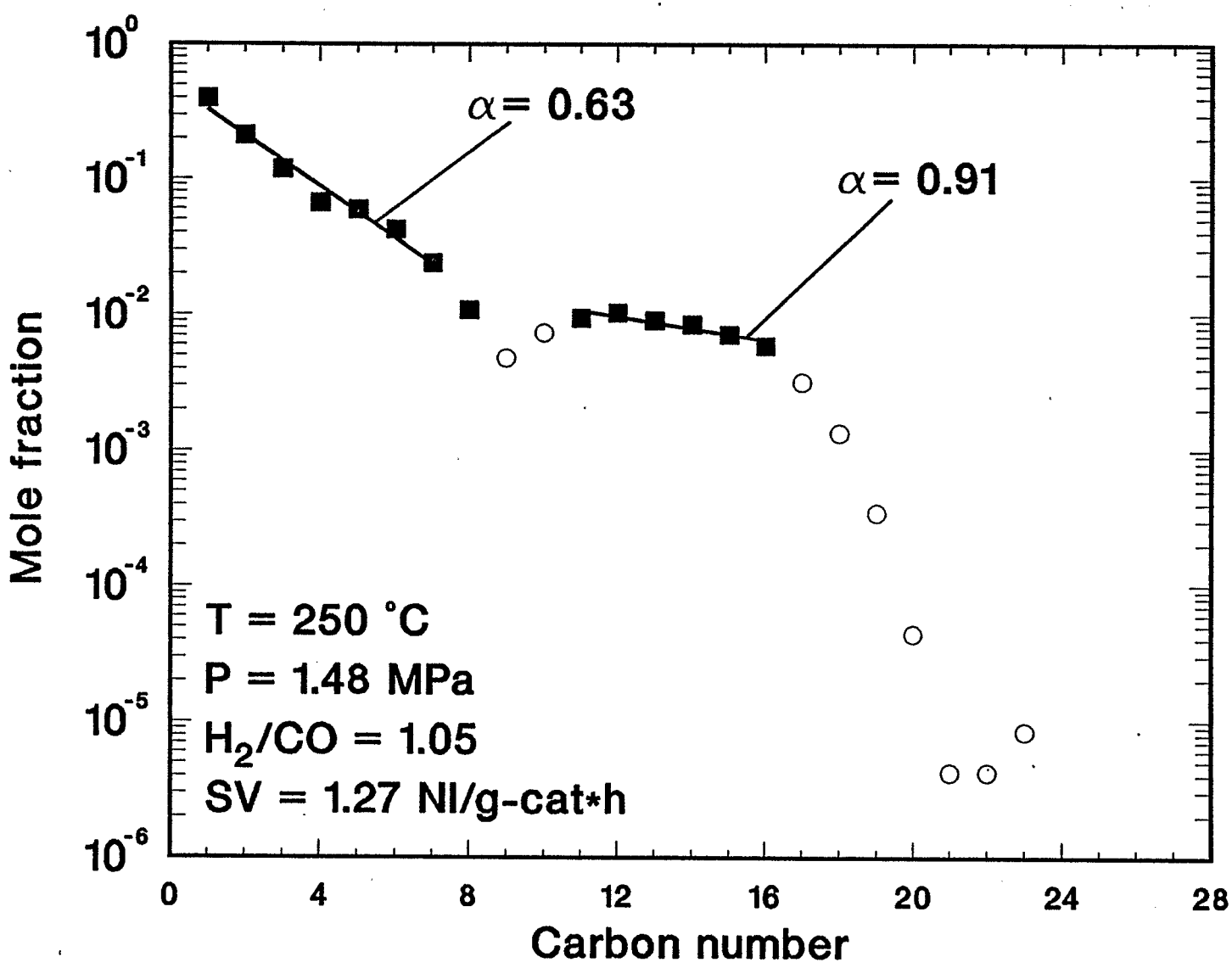

Figure 8. Anderson-Schulz-Flory plot for run FA-01-1687-4.

(The entire product spectrum was not analyzed)

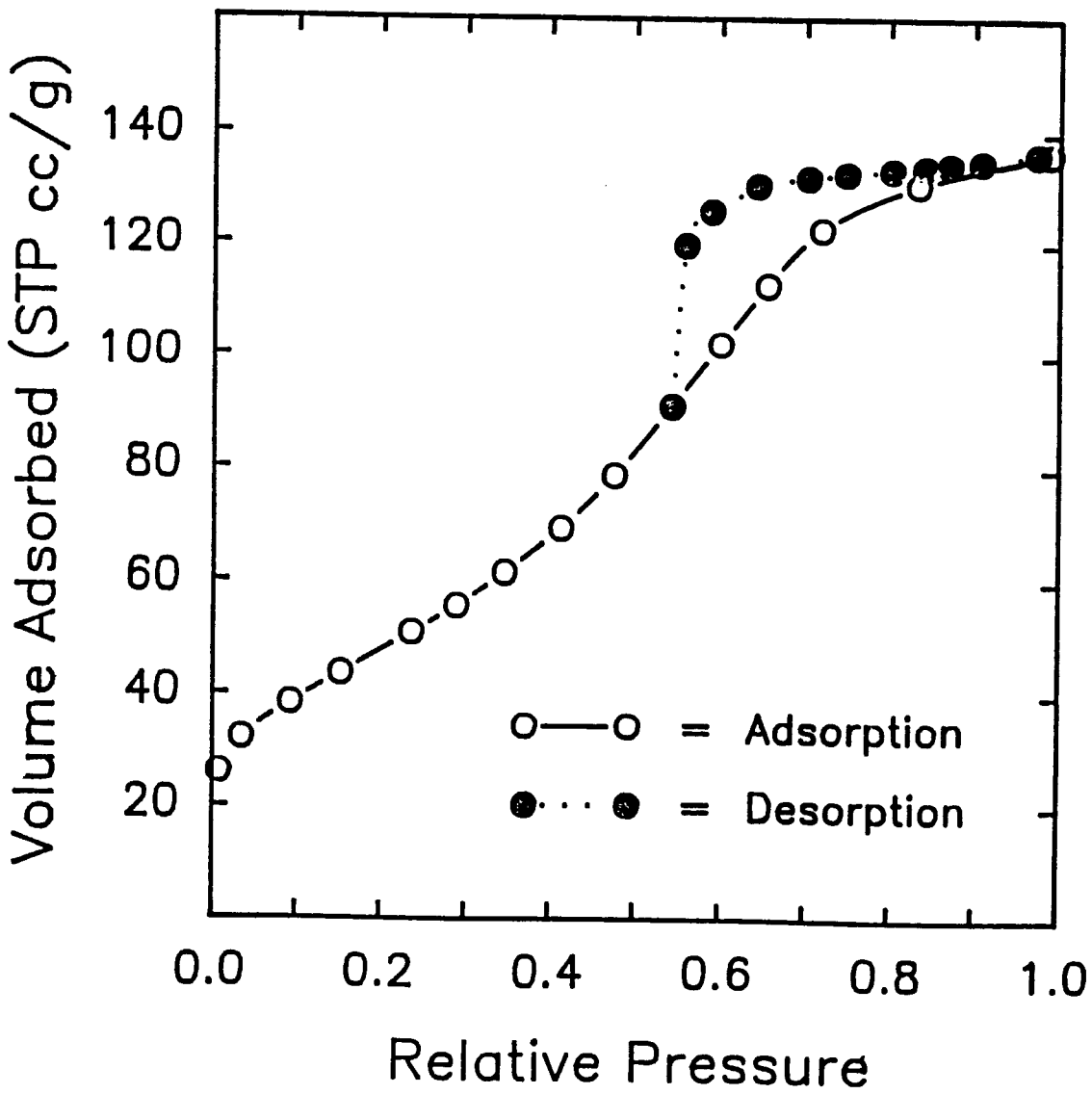

Figure 9. Adsorption/desorption isotherm for N_2 at -196 °C on an unpromoted $FeOOH/Fe_2O_3$ catalyst sample prior to calcination.

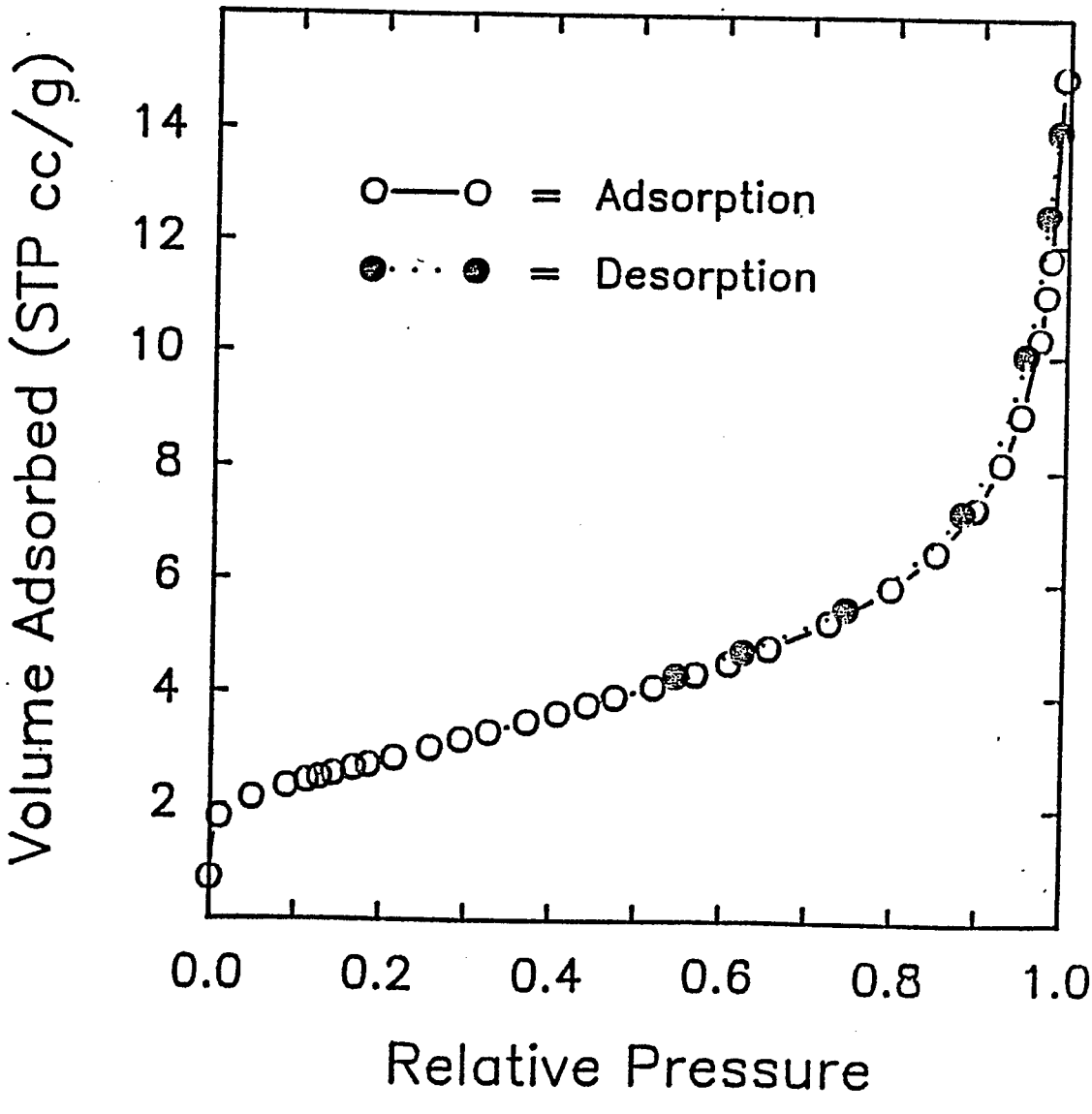

Figure 10. Adsorption/desorption isotherm for N_2 at -196 °C on an unpromoted $FeOOH/Fe_2O_3$ catalyst sample after calcination for 3 hrs at 300°C.

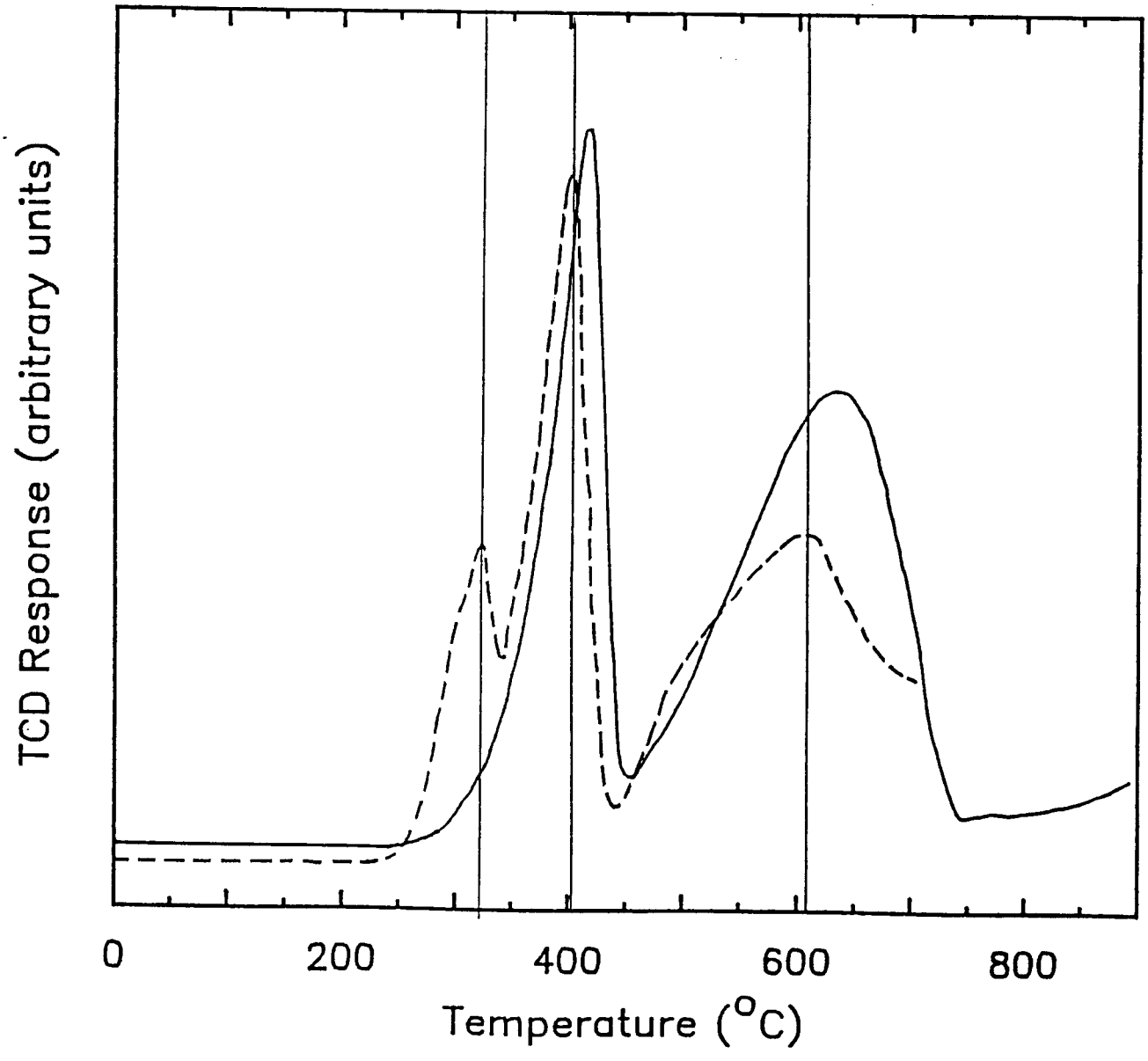

Figure 11. TPR profiles for unpromoted iron catalyst without prior calcination (dashed curve) and with prior calcination for 4 hrs at 300 °C (solid curve).

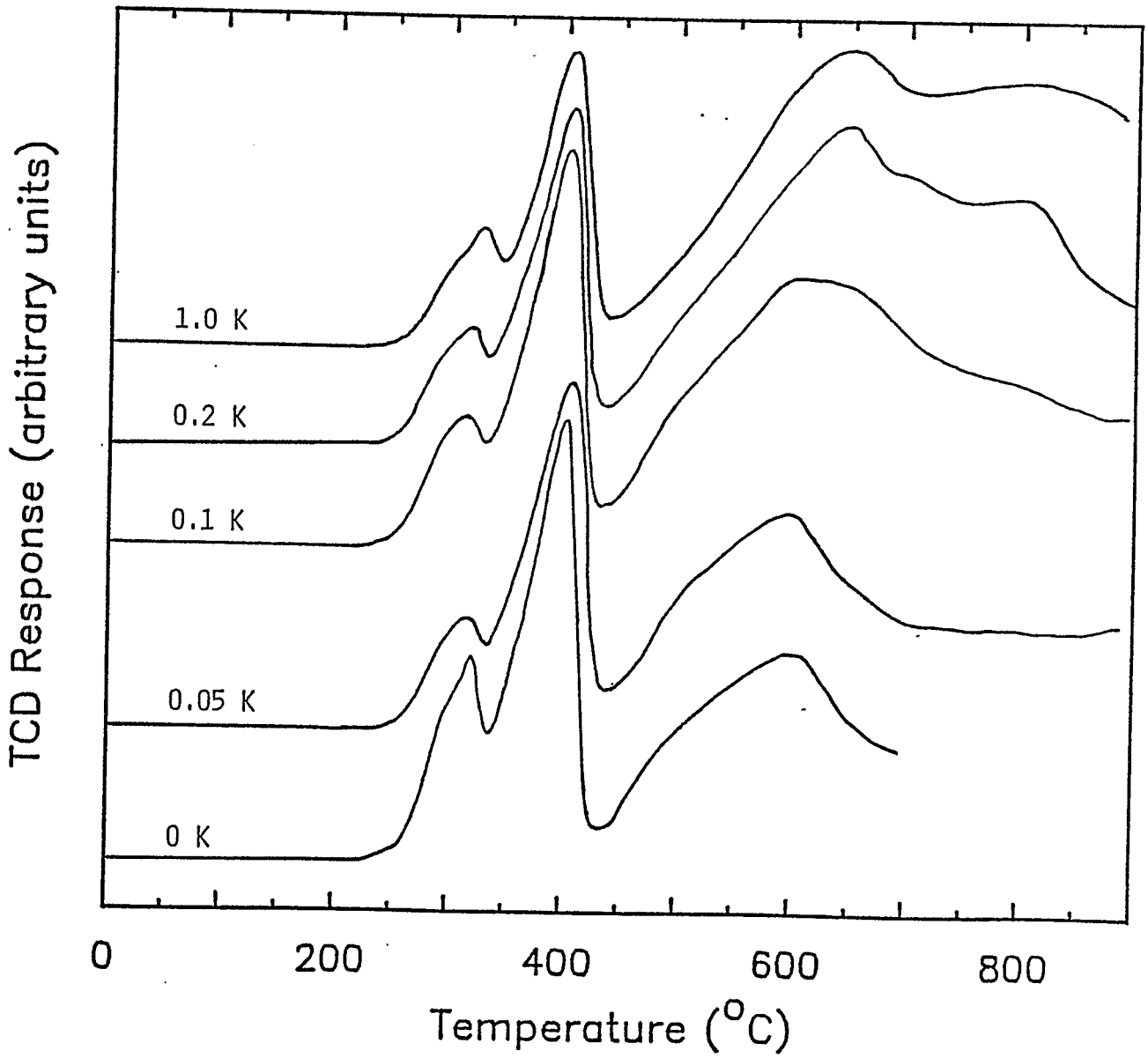

Figure 12. TPR profiles of copper–free, uncalcined iron catalysts containing the indicated levels of potassium promoter (in parts by weight per 100 parts of Fe).

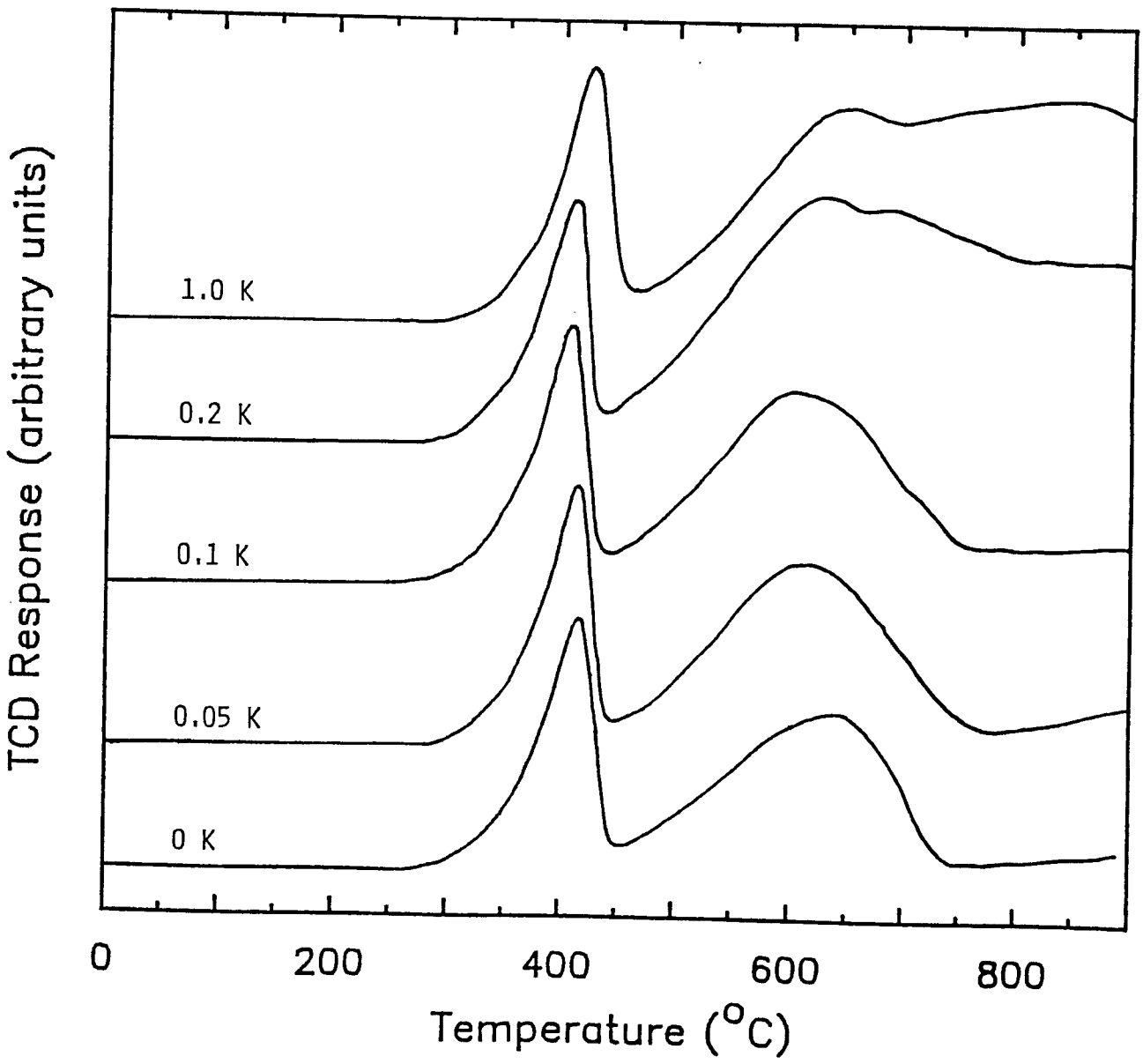

Figure 13. TPR profiles of copper–free, pre–calcined iron catalysts containing the indicated levels of potassium promoter (in parts by weight per 100 parts of Fe).

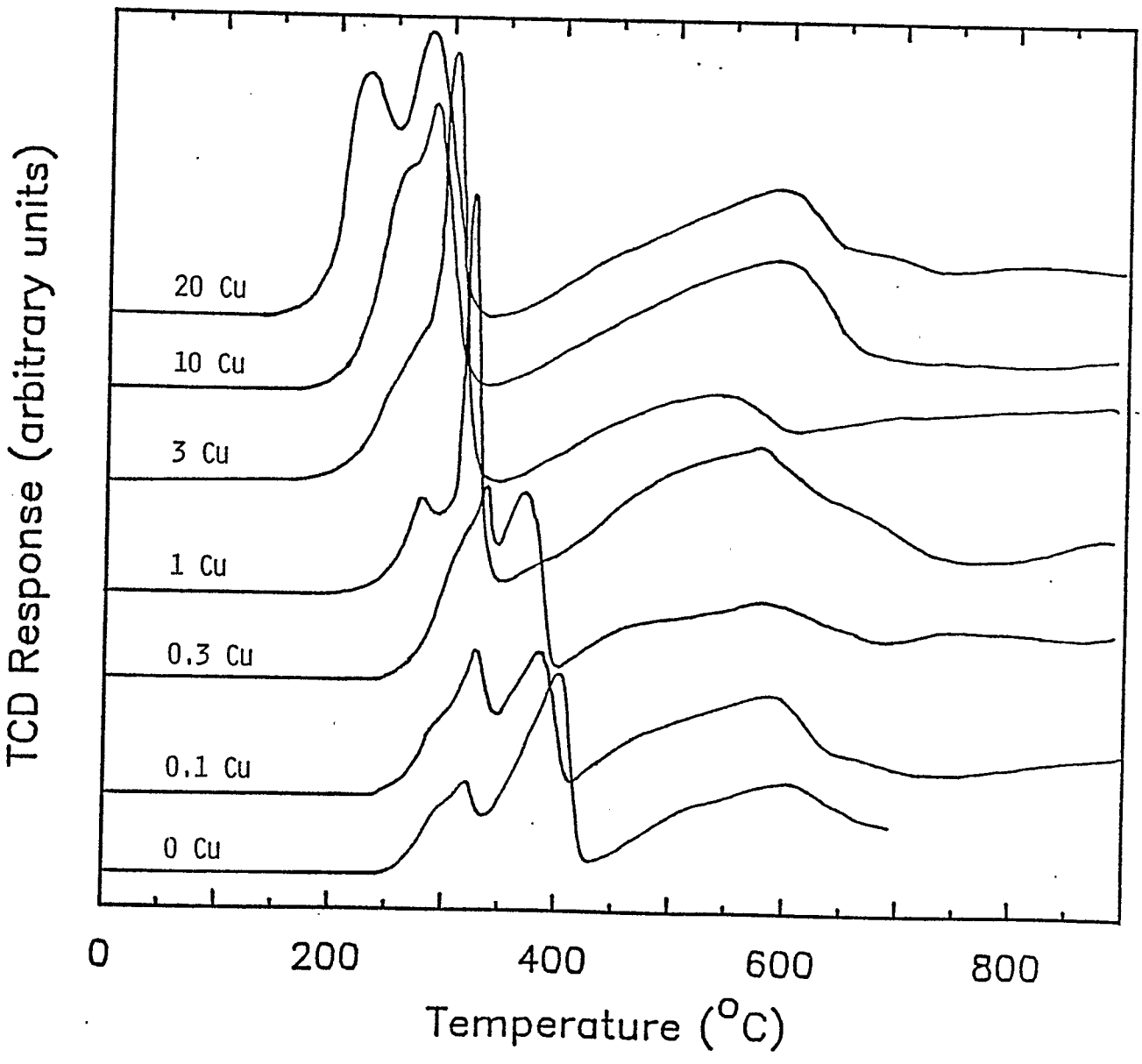

Figure 14. TPR profiles of potassium–free, uncalcined iron catalysts containing the indicated levels of copper promoter (in parts by weight per 100 parts of Fe).

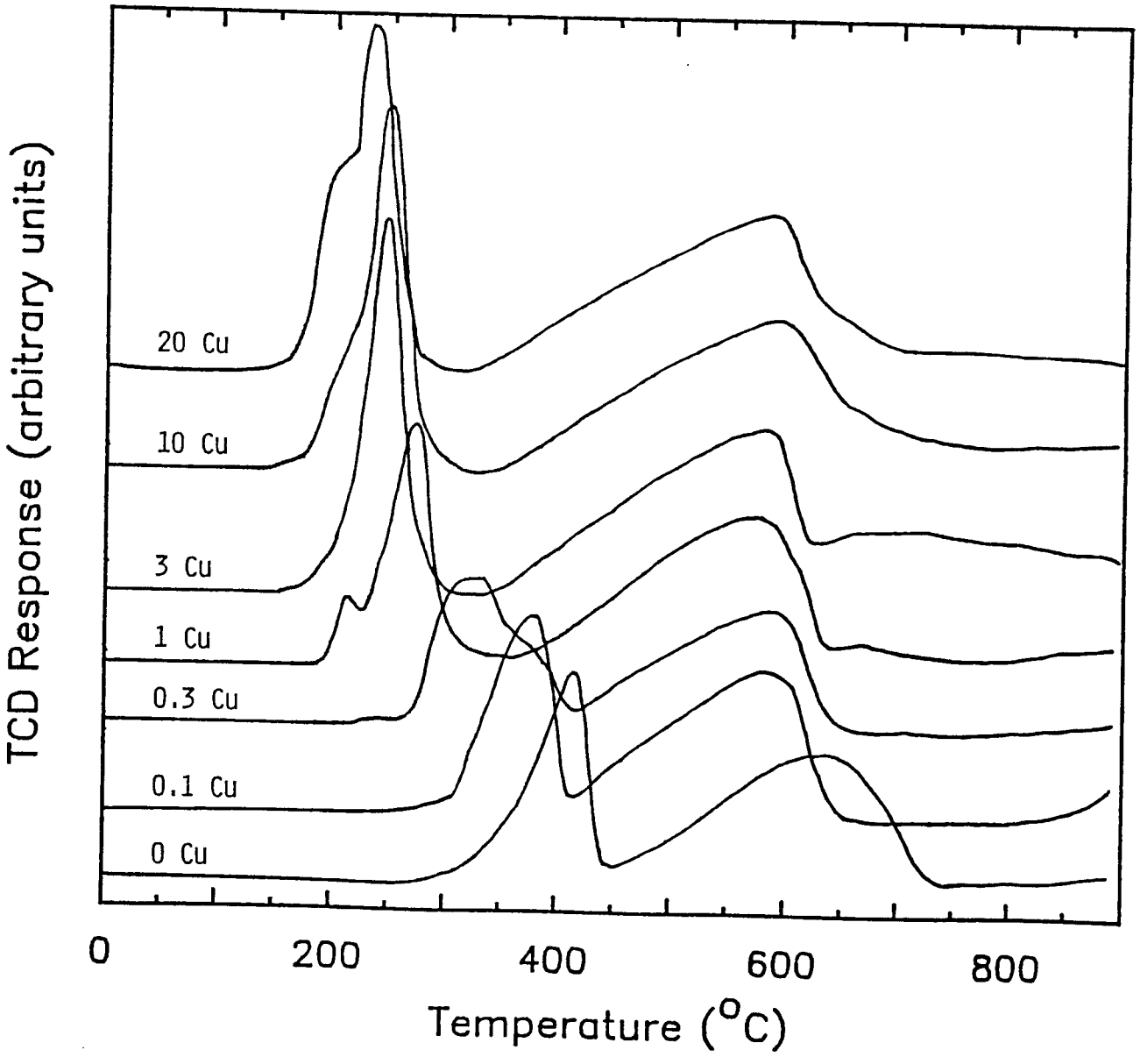

Figure 15. TPR profiles of potassium-free, pre-calcined iron catalysts containing the indicated levels of copper promoter (in parts by weight per 100 parts of Fe).

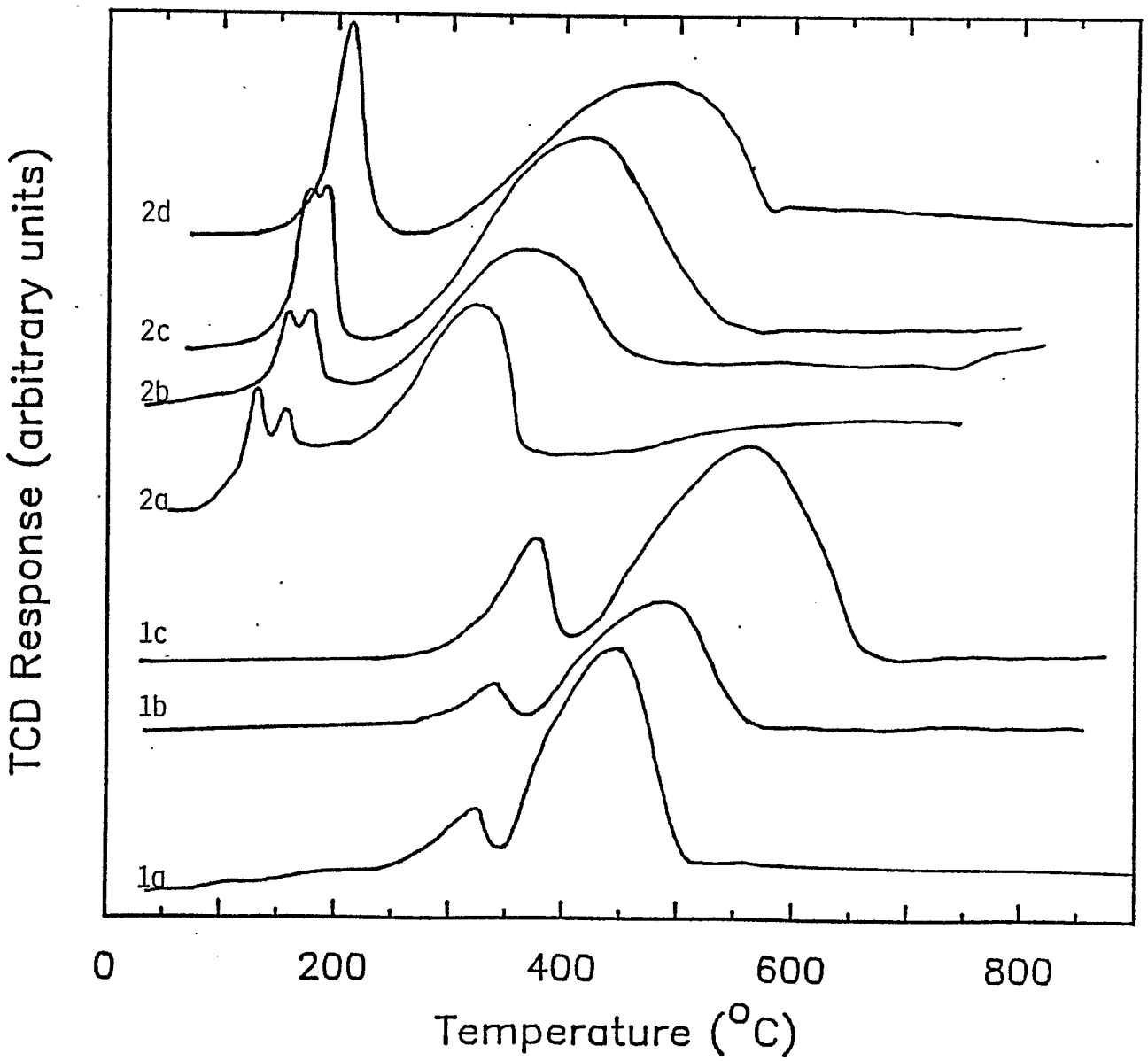

Figure 16. TPR profiles of unpromoted (1a, 1b, 1c) and copper–promoted (2a, 2b, 2c, 2d) (3 Cu/100 Fe) iron catalysts at the following temperature program rates (in °C/min): 1a, 3.4; 1b, 6.7; 1c, 20.4; 2a, 0.9; 2b, 3.2; 2c, 6.6; 2d, 20.1.

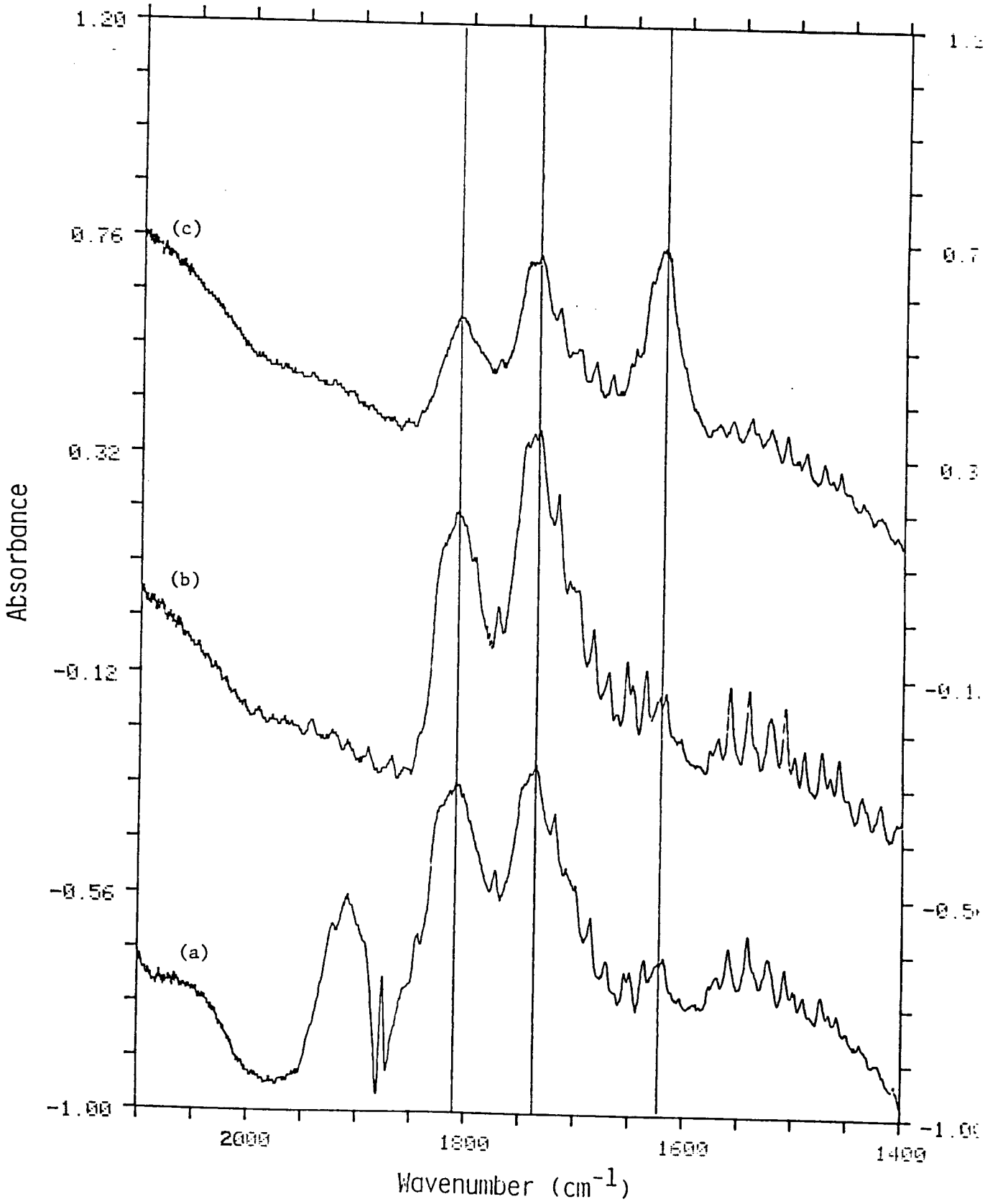

Figure 17. FT-IR spectra of NO adsorption on a reduced, unpromoted iron catalyst: (a) after admission of 12 torr of NO; (b) after evacuation of NO; (c) after admission of 25 torr of O_2.

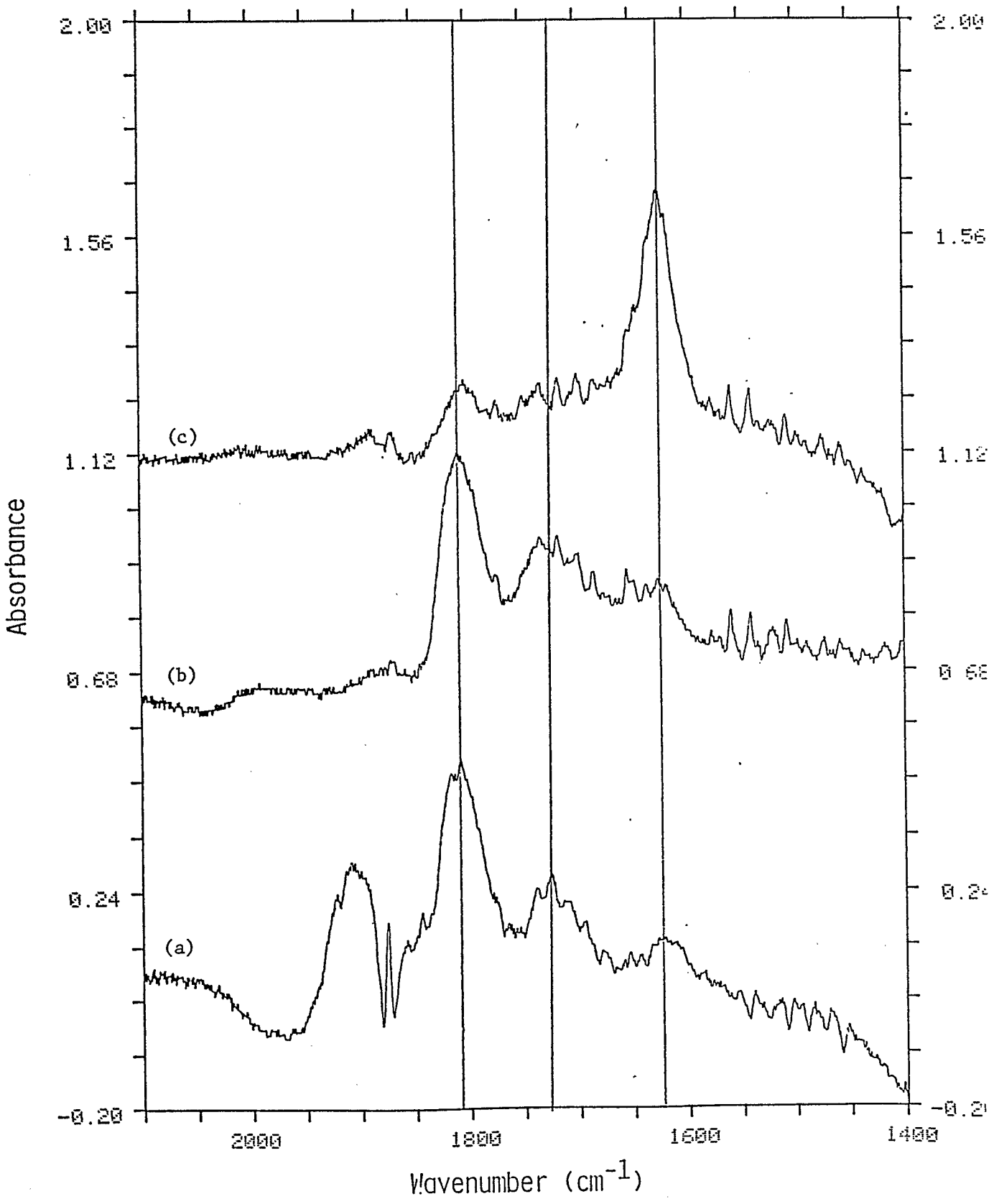

Figure 18. FT-IR spectra of NO adsorption on a reduced, potassium–promoted iron catalyst (1 K/100 Fe): (a) after admission of 12 torr of NO; (b) after evacuation of NO; (c) after admission of 25 torr of O_2.

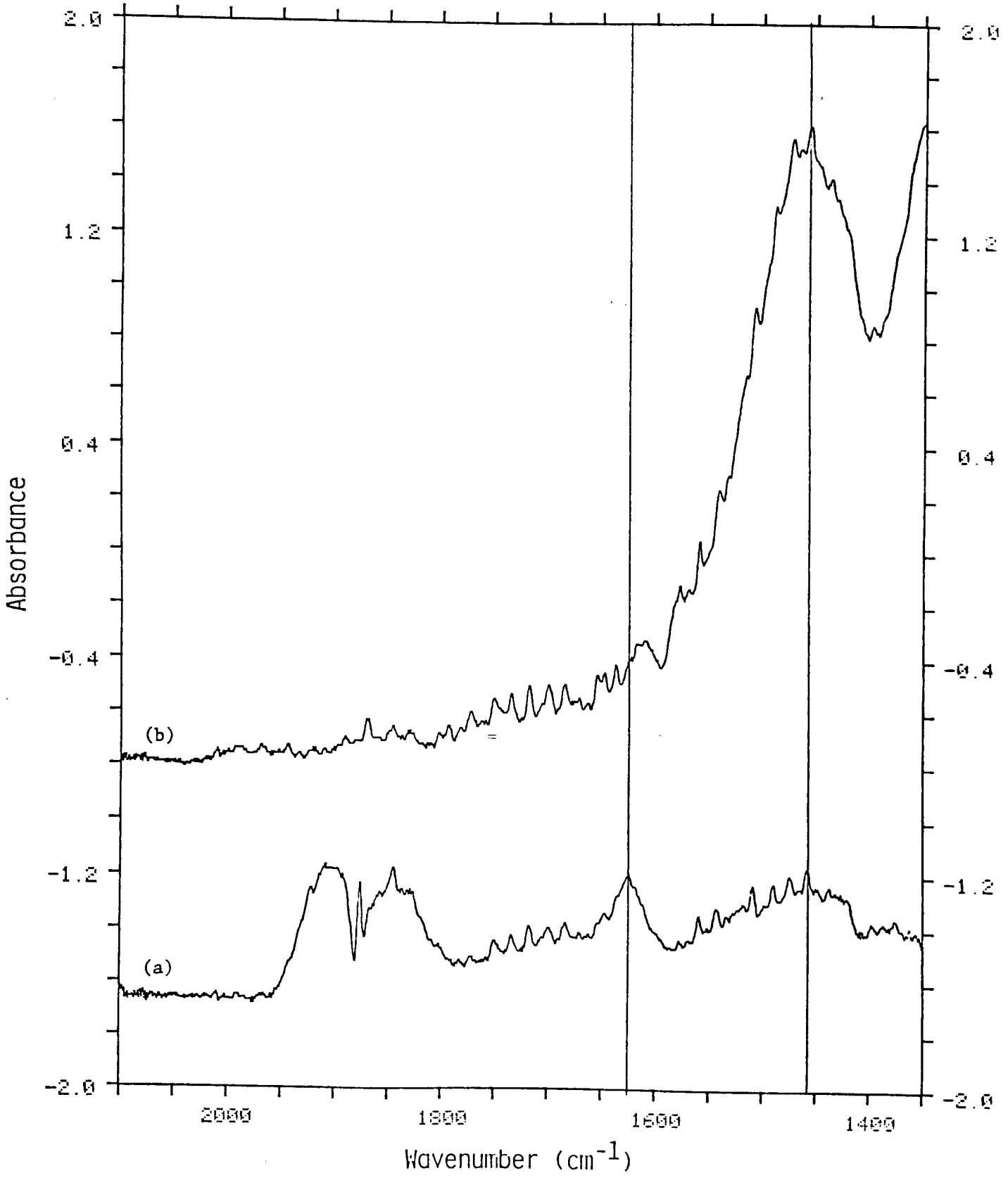

Figure 19. Continuation of Figure 18: (a) after admission of 12 torr of NO; (b) after evacuation of NO.

Appendix I. Catalyst Reduction Procedure

(a) Reduction Procedure for a Fused Iron Catalyst

The fused iron catalyst (United Catalysts, Inc., C73-1) was activated in situ with pure hydrogen at a space velocity of 20,000 h^{-1} (volume of gas at STP/(volume of catalyst h)) and atmospheric pressure at the outlet. The time-temperature schedule is listed in Table I.

Table I. Time-Temperature Schedule for Reduction

Temp. (°C)	Rate, °C/h	Duration, h
20 - 150	120	1
150	0	2
150-370	120	2
370	0	24
370-400	~300	0.25
400	0	24
430-235	(*i*)	(*i*)

(*i*) Natural cooling rate

After the reactor had cooled to the desired operating temperature, the ($CO+H_2$) mixture was introduced at 60 psig. The pressure was slowly increased in increments of 50 psig every two hours until the desired system pressure was attained.

(b) Reduction Procedure for a Precipitated Iron Catalyst

The precipitated iron catalyst used in run FA-02-1687 was reduced in situ in a fixed bed reactor according to the following procedure. The catalyst was first heated to 200°C in helium at a space velocity of 3140h^{-1} (based on catalyst volume) and atmospheric pressure. Following this the synthesis gas with H_2/CO ratio of 0.7 was employed at the same flow rate

and the catalyst temperature was raised to 280°C at a rate of ~20°C/h. The bed temperature was maintained at 280°C for the next 8 hours, and then the system was cooled to 235°C using a helium purge. After the catalyst was exposed to synthesis gas with H_2 CO ratio of 1:1 at a space velocity of 2.51 Nℓ/g-cat/h ($3{,}140h^{-1}$) and pressure of 50 psig. The pressure was increased in increments of 50 psig every two hours to the desired operating pressure of 200 psig.